A comparative study of total alkalinity and total inorganic carbon near tropical Atlantic coastal regions

Bonou Frédéric [1, 2, 8, *], Medeiros Carmen [7], Noriega Carlos [3], Araujo Moacyr [3, 4],
Hounsou-Gbo Aubains [5], Lefèvre Nathalie [6]

[1] Laboratoire de Physiques et Applications, LPA/ Université Nationale Des Sciences Technologies, Ingénierie Et Mathématiques (UNSTIM), Cotonou, Benin
[2] International Chair in Mathematical Physics and Applications (ICMPA-Unesco Chair), Université d´Abomey-Calavi (UAC), Cotonou, Bénin
[3] Center for Studies and Tests On Risk and Environmental Modeling (CEERMA), Federal University of Pernambuco (UFPE), Av. Arquiterura s/n, Recife, 50740-550, Brazil
[4] Brazilian Research Network On Global Climate Change, Rede CLIMA, S. José Dos Campos, SP, Brazil
[5] Instituto de Ciências do Mar (LABOMAR), Universidade Federal do Ceará (UFC), Av. da Abolição, 3207, CE: 60165-081, Fortaleza, Brazil
[6] Université Pierre Et Marie Curie, 4 place Jussieu, 75252 Cedex 05, Paris, France
[7] Laboratório de Oceanografia Física Estuarina e Costeira (LOFEC/DOCEAN/CTG), Federal University of Pernambuco, Av. Arquiterura s/n, 50740-550, Recife, Brazil
[8] Institut de Recherches Halieutiques et Océanologiques du Bénin, IRHOB, Cotonou, Benin

* Corresponding author : Frédéric Bonou, email address : fredericbonou@yahoo.fr

Abstract :

This paper is based on a comparison of the carbon parameters at the western and eastern borders of the tropical Atlantic using data collected from 55 cruises. Oceanic and coastal data, mainly total alkalinity (TA), total dissolved inorganic carbon (CT), sea surface salinity (SSS) and sea surface temperature (SST), were compiled from different sources. These data were subdivided into three subsets: oceanic data, coastal data and adjacent to the Brazilian (western) and African coastal areas (eastern) data. Significant differences between the TA data (2099.4 ± 286.4 µmol kg−1) at the western and eastern edges (2198 ± 141.9 µmol kg−1) were observed. Differences in the CT values between the western edge (1779.6 ± 236.4 µmol kg−1) and eastern edge (1892.2 ± 94.2 µmol kg−1) were also noted. This pattern was due to the different variabilities in the carbon parameters between the eastern and western border coastal areas and to the biogeochemistry that drives these parameters. In the western coastal area, the physical features of the continental carbon and oceanic waters mixing with the freshwater that flows from the Amazon and Orinoco Rivers to the South American coast are different than the physical features of the water that flows from the Congo, Volta and Niger Rivers in the eastern region. Applying the TA empirical relationship to TA with values of SSS < 35 in the western and eastern regions leads to a higher root mean square error (rmse) in the eastern and western regions. Therefore, most of the existing TA empirical relationships are most useful at the regional scale due to the difference in the water properties of each region. The relationships of TA and CT determined in the western and eastern regions do not reproduce in situ data well, especially at the adjacent edges. This difference is explained by the difference between the African and Brazilian coasts in terms of their carbon parameter characteristics and processes

responsible for their variation. Based on the mixing model, it has been shown that the primary productivity in the eastern region is higher than that in the western region. This is one of the reasons why the carbon parameters are higher in the eastern region. For each region studied, an equation for TA is introduced in this study.

Highlights

- Compiled three decades of carbon data cruises.

- Investigated TA/C_T differences in tropical Atlantic coastal zones.

- Significant difference between TA/C_T data from the African and Brazilian coastal areas were determined.

- High influence of C_T in the eastern region compared to that in the western region of the tropical Atlantic Ocean was recorded.

- Four empirical equations were proposed for the four regions studied.

1. Introduction

Between the African and South American continents, the tropical Atlantic receives approximately 0.1 Pg C yr^{-1} of carbon, 0.046 Pg C yr^{-1} of dissolved organic carbon (DOC), and 0.053 Pg C yr^{-1} of dissolved inorganic carbon total (C_T) (Huang et al., 2012). According to Araujo et al. (2014), 13.2% of the C_T and 27.3% of the DOC global values are transported from rivers into the world's oceans. Furthermore, rivers provide 0.8-1.33 Pg C to oceans worldwide, of which ~ 0.53 Pg C is transported from tropical rivers (30°N- 30°S) to adjacent estuarine-coastal systems (Huang et al., 2012).

In the tropical Atlantic, the Amazon River is the largest river, flowing from west to east, while the Congo River is the second largest river, which has a local dynamic in this area (Cai et al., 2008). The transport of terrestrial, oceanic and atmospheric carbon in the global carbon cycle is influenced by rivers. Freshwater is generally rich in terrestrial and atmospheric carbon and is transported to the ocean through rivers (Araujo et al., 2014). The high nutrient concentrations transported by the river flux within the continental shelf and adjacent oceanic region increase primary production and can lead to the absorption of CO_2 (Körtzinger, 2003; Regnier et al., 2013). Previous studies have

also revealed that South American estuaries (western region) and African estuaries (eastern region) are carbon sources ($+10.6\pm7$ mmoles m^{-2} day^{-1} and $+7.0$ mmoles m^{-2} day^{-1}, respectively) for the tropical Atlantic (Araujo et al., 2014). Therefore, the coastal regions adjacent to rivers are regions with highly variable CO_2 parameters due to the carbon input that occurs through the discharge of rivers into oceanic regions. The amount of carbon from the continental input at the separate edges (eastern and western) can influence the carbonate system, such as the total alkalinity (TA) and total dissolved inorganic carbon (C_T). It is necessary to collect data at these edges to better understand the variability of these parameters.

Important processes can be responsible for carbonate chemistry changes in the ocean, and they can be described by considering the changes in C_T and TA. The invasion of CO_2 from (or the release of CO_2 to) the atmosphere increases (or decreases) C_T while TA remains constant, leading to a rise and drop of [CO_2], respectively, with opposite changes in pH (since CO_2 is a weak acid). Respiration and photosynthesis led to the same trends, except that TA changed slightly due to nutrient release and uptake. $CaCO_3$ precipitation decreases C_T and TA at a ratio of 1:2 and, counterintuitively, increases [CO_2], although inorganic carbon is reduced.

The spatial distribution of CO_2 and C_T in the surface ocean is mainly explained by the temperature-dependent solubility of CO_2 on interannual timescales. Because of increased solubility at low temperatures, warm low-latitude surface water retains less CO_2 (~10 μmol kg^{-1}) and C_T (~2000 μmol kg^{-1}) than cold high-latitude surface water (CO_2 ~ 15 mol kg^{-1} and C_T ~ 2100 mol kg^{-1}). Significant deviations from these broad trends may occur locally and on seasonal time scales due to changes in salinity and processes such as biological activity, upwelling, temperature variations, river runoff, and other activities that alter C_T and TA.

Some equations have been developed in recent decades to determine the carbon parameters TA, C_T and fugacity (fCO_2) as functions of physical and other parameters that are easily measurable and

3

accessible (Takahashi et al., 2014, Lefèvre et al., 2010, Koffi et al., 2010). Linear regression relationships can be a good option to estimate carbon parameters. Empirical equations also present large uncertainties in data due to the complexity of the carbon parameters in coastal areas. Although empirical equations are useful to reproduce carbon parameters, they have spatial and temporal limitations for reproducing carbon parameters well in a whole oceanic basin. There have been few studies that focus on the tropical Atlantic with an emphasis on the contribution of river discharge to carbon. In 2006, other authors used the relationship TA vs. SSS (sea surface salinity) and SST (sea surface temperature) in the tropical Atlantic (30°S-30°N) for oceanic regions with the SSS criterion (greater than 31) (Lee et al., 2006). This empirical relationship cannot be used for data with low SSS in these regions with higher discharge due to major rivers. In the tropical Atlantic, Takahashi et al. (2014a) determined and used only one empirical relationship of TA regression for the whole tropical Atlantic basin; this relationship is similar to the one determined by Lefèvre et al. (2010), specifically for the Amazon region. In the same year, Koffi et al. (2010) determined a different TA relationship in the eastern Gulf of Guinea, with a slope that was highly different from that determined in Lefèvre et al. (2010) and Takahashi et al. (2014a). Due to the spatiotemporal variability, in the western region, an empirical relationship of C_T was obtained by Bonou et al. (2016a) using SSS and time variation (year), while in the eastern region, Koffi et al. (2010) determined an empirical relationship of C_T using SST and SSS (**Table 1**). It is desirable to continue studying the performance of linear regression, multiple regression or other methods to obtain a better estimation of the carbon parameters. The compilation of many data cruises, within the context of acquiring new observation data, is a good means to determine existing relationships in order to have robust equations that are adaptable to the regions, leading to smaller uncertainties.

Table 1

4

Data from different sources are compiled from different oceanographic data cruises (1983-2014) to compare the TA and C_T variations in the western and eastern tropical Atlantic, mainly in coastal areas adjacent to rivers. The compilation of several data cruises was used to test the reliability of the existing relationships and to reproduce the TA/C_T distribution in these transition regions. A comparative study was performed to emphasize the limits and differences in the variation in TA/C_T at the tropical Atlantic borders.

2. Material and Methods

2.1. Database and methodology

All available cruise data were extracted from oceanographic and voluntary merchant ships (20°S-20°N, 70°W-15°E) in the tropical Atlantic, which is the study area where in situ data TA, C_T, SST and SSS were sampled and measured (**Figure 1**). In Figure 1, the data are shown in red and green for SSS<35 (points in black indicate SSS>35). The dataset was acquired from 1983 to 2014 through 55 campaigns (**Table 2**) completed with those used in Bonou et al. (2016). Conductivity, temperature and depth data acquired with CTD and bottle samples during those surveys were obtained from the Carbon Dioxide Information and Analysis Center (http://cdiac.ornl.gov/oceans/bottle_discrete.html).

Figure 1 (Single Column)

Table 2

5

The TA and C_T data used in this study were obtained from data cruises and were determined by potentiometric titration from either a full curve ("Full") or a single-point ("1-point") titration. The SSS database was obtained from an updated version of SSS data from 2013 by Reverdin et al. (2007). These data were used as indicators for determination of the area affected by freshwater due to rivers in the tropical Atlantic. The monthly SST data were extracted from the Objectively Analyzed air-sea Fluxes Project (OAFlux) database (with 1° of longitude and 1° of latitude). The SST data used in this study were acquired from 1958-2014, and the data are available on the Woods Hole Oceanographic Institution (WHOI) website at oaflux.whoi.edu. The OAFlux project provides a synthesized product generated from the reanalysis datasets NCEP1, NCEP2, ERA40 and ERA (Yu and Weller, 2007, Yu et al., 2008).

The TA and C_T relationships used were determined by different authors (see **Table 1**) to verify their limits to reproduce data compared to the observation data, especially at the eastern and western borders.

2.2. Statistical analysis

Statistical analysis and the Mann–Whitney test were used to compare two sets of data (TA, C_T, SST, and SSS) from different areas (western tropical Atlantic and eastern tropical Atlantic) to determine the difference between the carbon parameters (TA and C_T) in the different localities. Linear regression methods were applied to determine and test the connections between the physical parameters and carbon parameters; this method was also used to observe the best fit that matched the observation data. To compare these different relationships, the root mean square error (rmse) was calculated as follows:

$$\text{rmse} = \left[\frac{1}{n-1} \times \sum_{i=1}^{n} \left(X_i - Y_i \right)^2 \right]^{\frac{1}{2}} \quad (3);$$

6

where Xi is the observed value and Yi is the modeled value at time/place i.

The Kruskal–Wallis test was used to identify significant differences ($\alpha=0.05$) between all regions. Additionally, Dunn's test was applied to identify significant differences between borders (NW, NE, SW, and SE, for $\alpha=0.05$) and between hemispheres.

3. Results

3.1. The distribution of SSS and SST anomalies in the tropical Atlantic

Standard deviations of SSS anomalies computed for the period from 1970-2013 using the database from Reverdin et al. (2007) actualized in 2013 allowed us to map the areas under distinct degrees of influence of freshwater input due to river discharge and/or precipitation (Figure 2). The regions presenting high SSS variability (SD>1) along South America corresponded to coastal areas adjacent to the mouths of the Amazon and Orinoco Rivers and areas along the African coastal border adjacent to the Congo, Niger and Volta River mouths. Lower variations in SSS anomalies were observed in the oceanic zone and along coastal areas not receiving large river discharge, as is the case for the NE-Brazilian coast and the northern coast of Africa. The São Francisco River in NE Brazil (**Figure 2**) does not induce significant variation in the SSS due to the presence of numerous dams of hydroelectric plants along its course, drastically reducing its flow despite the extension of its drainage basin.

Figure 2 (Single Column)

The SST distribution in the study area presents a seasonal zonal pattern with less variable values along the western Atlantic relative to that of the eastern Atlantic. SST along the South American coast varies from 26 to 28 °C in January and between 25 and 29 °C in July. Along the African

7

coast, SST is higher (>27 °C) in the eastern Atlantic (0° to 5°N) in January and lower (<26 °C) in coastal areas between the equator and 10°S in July (**Figure 3**).

Figure 3 (Single Column)

The annual amplitude of the SST in the western Atlantic (including 20°S-20°N; 70°W-30°W) was 3.0 °C. However, in the eastern Atlantic (including 20°S-20°N; 20°W-15°E), the amplitude of the SST was 5.7 °C (**Figure 3,4**).

Figure 4 (1.5 Column)

A subset division of the tropical Atlantic Ocean into four regions (NW, SW, NE and SE) is included according to the variability in the SST climatological. This division sought to differentiate the variations between the hemispheres and the continental borders (**Figure 4**).

The Kruskal–Wallis test showed significant differences (α=0.05; p=0.0007) between all regions. Additionally, Dunn's test showed significant differences between borders (NW $\neq$ NE; α=0.05; p=0.012 and SW $\neq$ SE; α=0.05; p=0.008) and between hemispheres (NW $\neq$ SW; α=0.05; p=0.009 and NE $\neq$ SE; α=0.05; p=0.003).

For SSS<35 (freshwater influence), the statistical test also confirmed a significant difference between the SST values of the eastern and western regions (Mann–Whitney test, p=0.0001; α = 0.05).

3.2. TA and C_T in the tropical Atlantic

Three hundred ninety-two in situ coastal data samples of TA, C_T, SSS and SST from the western region, represented in red, were used in this study and compared to 103 data samples of TA, C_T,

8

SSS and SST from the eastern region, represented in green (**Figure 1**). All these data were obtained under the criterion of SSS being less than 35 psu. A significant difference was observed when the selected TA and C_T data (in red points) from the western Atlantic were compared with TA and C_T data (green points) from the eastern tropical Atlantic. At the western edge, the average value of TA (2099.4 ± 286.4 µmol kg^{-1}) was obtained; this value was lower than the value obtained from the eastern tropical Atlantic (2198 ± 141.9 µmol kg^{-1}) (**Table 3**), while the standard deviation indicated a higher variation in TA in the western region than that obtained in the eastern region (Mann–Whitney test, $p = 0.0008$, $\alpha = 0.05$). For the C_T variable, (1892.2 ± 94.2 µmol kg^{-1}) and (1779.6 ± 236.4) µmol kg^{-1} are the mean values and the standard deviation obtained, respectively, at the eastern and western borders. The standard deviation on CT in the western border was higher than that of the eastern border, showing higher variation in TA and CT in South America than in the African border (Mann–Whitney test, $p = 0.00002$, $\alpha = 0.05$).

Table 3

This result supports the higher average values of TA and C_T (**Table 3**) in the eastern region Koffi et al. (2010) and the higher TA and CT values in the Gulf of Guinea, especially in this upwelling region (**Figure 4**).

3.3. Relevance and limitation of existing relations for TA and C_T in the tropical Atlantic.

The relationships proposed by Lefèvre et al. (2010), Koffi et al. (2010) and Bonou et al. (2016a) (**Table 4**) were used to compute TA and C_T and to observe their spatial relevance and limitations in the tropical Atlantic. The data in red and green samples have SSS values lower than 35, while the data in black correspond to those of the regions where SSS is higher than 35 (**Figure 1**).

Table 4

Observations of SSS<35 in the western border are due to the higher influence of rivers and freshwater due to the retroflexion of Amazonian waters by the North Brazilian Current (NBC) and into the NECC, which is beyond the influence of rainfall in the equatorial region due to the ITCZ (intertropical convergence zone). In this region, the empirical relationship proposed by Lefèvre et al. (2010) represents the TA observations better than the relationships proposed by Koffi et al. (2010) (**Figure 5A**). The standard deviation of TA from Lefèvre et al. (2010) was 28.6 μmol.kg^{-1}, while that obtained for TA by Koffi et al. (2010) was 64.8 μmol.kg^{-1} (**Table 4**). The greatest discrepancies occur for data with SSS<30.

Figure 5 (Single Column)

The opposite trend was observed in the eastern region, where the relationship described in Koffi et al. (2010) is better at reproducing the observation data than that described in Lefèvre et al. (2010) (**Figure 6**). The rmse value of TA was 12.5 μmol kg^{-1}, which was obtained from the relationship from Koffi et al. (2010) in the eastern region. This rmse value TA is almost two times lower than that obtained with the relationship of Lefèvre et al. (2010) (**Table 4**). This result agrees with that obtained in Lefèvre et al. (2010), which showed the best fit of TA with SSS when using Koffi et al. (2010).

Figure 6 (1.5 Column)

3.4. Biological processes

10

In the western and eastern tropical Atlantic, biological consumption is one of the processes that influences the variation in the carbon parameters around tropical edges (Cooley et al., 2007; da Cunha et al., 2013; Araujo et al., 2014).

As explained above, the surface C_T concentration is influenced by lateral and vertical mixing of water with different levels of C_T (the transport effect), photosynthesis and oxidation of organic matter (the biological effect) and changes in temperature and salinity (Takahashi et al., 1993; Lee et al., 2000). However, these effects are directly or indirectly correlated with SST, but the trends often differ seasonally and geographically.

According to Koffi et al. (2010), equatorial upwelling and coastal upwelling along the eastern boundary merge to form a cold tongue during the main upwelling season, and the cold tongue undergoes advection westward by the South Equatorial Current (SEC). This cold tongue transports CO_2-rich waters, and fCO_2 increases as the surface water temperature increases toward the west. The Guinea Current (GC) and SEC are influenced by several fluvial contributions, including the Volta River (4°N-0°), Niger River (3°N, 8°E) and Congo River (-6°S, 12°E) (Koffi et al., 2010). The eastern border is strongly affected by biological activity (NE and SE). The average C_T was 2056 μmol kg^{-1}, which is close to that of the Atlantic Ocean, as indicated by Millero (2006).

The satellite data through the MODIS-Aqua sensor were used for the study region. The highest concentrations of chlorophyll-*a* are observed in the coastal regions near the Amazon River, Orinoco River, Congo River and NW Africa (coastal upwelling) (**Figure 7**).

4. Discussion

4.1. Analysis of the regions influenced by tropical Atlantic Rivers

The standard deviation distribution of anomalies was used by Bonou et al. (2016a) to identify regions with higher variations in the variables considered. In our work, this method was applied to investigate the subregions of the tropical Atlantic characterized by higher variations in SSS (**Figure 2**). The fact that almost all the regions of the tropical Atlantic presenting large SDs of SSS anomalies were located near tropical rivers presenting high discharge corroborates that this method is robust to identifying the influence of its discharge on salinity.

The standard deviation of SSS was an anomaly with values between 0.2 and 2.0 for the coastal regions of the study area. There is a significant difference between the SSS anomalies (Mann–Whitney test, p=0.0005; $\alpha = 0.05$) at the western and eastern borders of the tropical Atlantic. The hydric balance of the Amazon and Orinoco Rivers at the western edge is greater than the balance of the Congo, Niger and Volta Rivers at the eastern border (Dai and Trenberth, 2002; Cai et al., 2008; da Cunha et al., 2013; Araujo et al., 2014). According to Bonou et al. (2016a), in the tropical Atlantic, the variation in SSS is higher in the western region, with SSS values between 1 and 38.

The western tropical Atlantic shows a higher variability in SSS and a less pronounced seasonal variability in SST. On the other hand, the eastern tropical Atlantic presents a lower variability in SSS but a strong seasonal variability in SST (**Figures 2, 3 and 4**). This area experiences coastal upwelling (Schneider et al., 1997; Dale et al., 2002), where a rise in cold-water masses rich in nutrients and CO_2 is observed and surface coastal water is pushed offshore by Ekman divergence. The SSS is a physical parameter that has a high correlation with carbon parameters, and its variability is believed to impact carbon parameters. In the Tropical Atlantic, the SSS is highly correlated with TA and CT (Bonou et al. (2016a), Koffi et al. (2010), Lefèvre et al. (2010); therefore, the stronger influence of the Amazon and Orinoco Rivers in the western tropical Atlantic is one explanation for the difference observed in the carbon parameters between the eastern and western regions.

12

4.2. Pertinence of existing relations to the tropical Atlantic.

The results presented in **Figures 5A** and **5B** show that the relationships from Lefèvre et al. (2016) are adapted in the western tropical Atlantic region mainly in the Amazon and Orinoco Rivers, while the relationship from Koffi et al. (2010) reproduces the observations in the eastern tropical Atlantic well, mainly in the Gulf of Guinea.

In the central basin of the tropical Atlantic, the results with SSS≥35 showed that the behavior was very close between the two empirical relationships (**Figure 5C**). The relationship from Lefèvre et al. (2016) had a slightly higher rmse value than that obtained from the relationship from Koffi et al. (2010) (20.5 and 19.2 μmol kg^{-1}, respectively). According to these results, the use of the two empirical relationships yielded similar TA values in the central region when SSS≥35 psu.

Almost all TA data with SSS≥37 are clustered around the green line, which is the line represented by the relationships from Koffi et al. (2010). Data with SSS≥37 are located in the SEC region (**Figure 6**), which extends to the western part. This result means that the relationship from Koffi et al. (2010), as determined in the eastern region, can be extended into the western part of the SEC. Analysis of the proposed relationships used to determine C_T is more complicated, at least regarding its graphical representation. In the eastern region, Koffi et al. (2010) determined C_T relationships using SSS and SST, while Bonou et al. (2016a) determined a C_T relationship using only the SSS function but still considered its temporal variation (**Table 3**) in the western tropical Atlantic region. The C_T relationships in both regions (western and eastern) do not depend only on SSS and TA relationships. In this case, C_T cannot be estimated only as a function of a single SSS parameter, and the statistical results are presented in **Table 4** (Bonou et al., 2016b).

13

In the western tropical Atlantic, the rmse value was obtained from the estimated C_T derived from Bonou et al. (2016a), and this value was 41.1 µmol kg^{-1} considering that the relationship from Koffi et al. (2010) gives 47.9 µmol kg^{-1} as the rmse value. In the eastern region, the rmse value obtained from the estimated C_T relationship from Koffi et al. (2010) was 28.11 µmol kg^{-1}, while from Bonou et al. (2016a), the rmse value was 29.6 µmol kg^{-1}. In the oceanic region (SSS$\geq$ 35), the rmse values were also similar between the two empirical relationships (34.7 and 35.1 µmol kg^{-1} for Koffi et al. (2010) and Bonou et al. (2016a), respectively). In fact, the greatest variation in SST observed in the eastern edge of the basin contributes to the C_T equation since SST is one of the key state variables that influence the carbon cycle in this region (Lefèvre et al., 2008; Koffi et al., 2010, Bonou et al., 2016b). On the other hand, the empirical relationships of C_T proposed for the western edge do not consider SST because their variation is lower at the western edge than in the eastern region (Lefèvre et al., 2010; Ibánhez et al., 2015; Bonou et al., 2016a). According to Key et al. (2004), the surface C_T distribution is affected by physical processes; however, the pattern is more similar to that of nutrients (e.g., nitrate) than to that of salinity. This is because C_T concentrations are more strongly affected by biology than TA concentrations.

4.3. Lithological composition of basins and influence of plumes

The different rock types that dominate the river basins influence the input of CO_2 through rock weathering and through riverine transport of inorganic carbon to the ocean. The chemical erosion of inorganic materials consists of dissolving or hydrolyzing primary minerals of rocks and soils. The chemical reactions require CO_2 and release C_T (mainly as HCO_3^-). Thus, different rock types have different CO_2 consumption rates. According to Amiotte-Suchet et al. (2003), high CO_2 consumption rates are observed in carbonate rocks, moderate CO_2 consumption rates are observed in basalts plus shales, and low CO_2 consumption rates are observed in shales plus and

14

sands/sandstones. Thus, the Amazon and Orinoco Rivers have high CO_2 consumption rates, and the Congo and Niger Rivers have moderate and low CO_2 consumption rates. Araujo et al. (2014) observed that the contribution of the mean CO_2 fluxes consumed by the total HCO_3^- river flux was 82 and 88% for the western border and eastern border, respectively. These authors also indicated that during a dry period, the atmospheric CO_2 flux consumed through rock weathering was lower than that during a more humid period. However, middle-latitude and subtropical larger rivers have high bicarbonate (HCO_3^-) concentrations and fluxes because of the abundant distribution of carbonate minerals in their drainage basins. In contrast, tropical larger rivers, such as the Amazon and Orinoco Rivers, have low HCO_3^- concentrations (Cai et al., 2010).

Large rivers also generate offshore plumes that are characterized by high buoyancy and biological productivity because of their low salinities, high levels of nutrients, and suspended and dissolved terrestrial materials (Higgins et al., 2006; Kouamé et al., 2009; Kang et al., 2013). As a result, the chemical, geological, biological and physical environments of the adjacent marginal seas are affected. Low-salinity regions at the eastern edge (SSS <35) in the Atlantic Ocean can be found in two regions according to Bakker et al. (1999): one north of the equator and one near the Congo River. Van Bennekom et al. (1978) and Vangriesheim et al. (2009) showed that the influence of the Congo River ranges from -3.5° to -6.5° latitude and reaches 6.5° E in the Atlantic Ocean (700 km offshore).

In the Atlantic Ocean, the dispersal of the Amazon River water leads to a brackish water plume that can exceed 10^6 km^2, reaching latitudes as far from the river mouth as 30°W (Coles et al., 2013) or even 25°W when the North Equatorial Countercurrent (NECC) is strong (Lefèvre et al., 1998). Recently, Ibánhez et al. (2017) compared the monthly precipitation rate with the monthly SSS in five regions of the tropical Atlantic. They found highly significant linear relationships of

15

precipitation with SSS across the western Atlantic basin. The extension of the Amazon River plume was highly significant, ranging from 0.25 to $1.60 \times 10^6 \, \text{km}^2$, after removing the influence of rainfall. In Tropical Atlantic regions, low salinity patches are related to large rivers, such as the Amazon (5413 km^3 year^{-1}), followed by the Congo (1263 km^3 year^{-1}) and Orinoco (1170 km^3 year^{-1}), spreading freshwater by surface oceanic circulation (Araujo et al. 2014).

According to Araujo et al. (2014), significant differences were observed between the large estuarine systems of the Atlantic Ocean. The authors indicated that C_T and TA showed significant differences between the eastern (Volta, Niger and Congo Rivers) and western (Orinoco, Amazon, São Francisco and Paraíba do Sul Rivers) estuaries. Other important parameters also showed significant differences, such as pCO_2 and dissolved organic carbon (DOC). According to these authors, DOC is higher in the eastern region; this would affect coastal concentrations in that region, increasing C_T levels in the adjacent coastal region. Additionally, TA is mainly affected by the chemical reactions of the different types of rocks in the soils of the hydrographic basins, which are carried to the coastal region via runoff

Based on the approaches of Ternon et al. (2000), Körtzinger (2003), Cooley and Yager (2006) and Araujo et al. (2014), a simple conservative mixing model was used to calculate the proportions of C_T in western rivers (Amazon and Orinoco) and eastern rivers (Niger, Volta and Congo) for plume water and seawater in a given plume sample (Figure 10). This mixing model approach has been widely detailed in the supplementary material of Araujo et al. (2014). It is assumed that the effects of precipitation and evaporation on the carbon and freshwater mass balances are small compared to the river (Cooley and Yager, 2006) over the first 10 m-deep plume. Additional variations in CT not attributable to mixing were then ascribed to biology (CTbio). Using the mixing equations of Araujo et al. (2014), we used TA, SSS and CT to estimate the excess or deficit of CTbio in the east and west coastal regions (TAbio calculation is not necessary here, as TA is considered a

16

conservative parameter). Positive values of ΔCTbio indicate an inorganic carbon deficit, implying

that the respiration process exceeds the respiration process. Thus, the system is considered to be

autotrophic, while negative CT values indicate excess CT, suggesting that respiration > production,

and the system is considered heterotrophic. The results showed that both regions had negative

CTbio values in the estuarine region, indicative of excess CT. Outside the plume, the values

oscillate between positive and negative; however, the mean values of the gradients indicate excess

CT. In the western region, 7% of the CT excess (bio) average across the entire saline gradient was

obtained, while in the eastern region, this percentage was lower (0.2%). According to these results,

the primary productivity in the eastern region is higher than that in the western region (Figure 10 a

and b). Additionally, we have to consider that the extension of the plumes differs, and the saline

values are smaller in the western region, generating a greater amplitude of variation between the

CT values. The concentrations of HCO_3^- (the main component of CT coming from the rocks) in

the eastern region are higher; however, the freshwater flow is greater in the western region. The

observed concentrations showed that the western region has an average CTbio excess of 92 μmol

kg^{-1}, while the eastern region has an average CTbio excess of 3 μmol kg^{-1}. In estuarine zones, these

excesses of CT are greater. In the western region, it reached 14%, while in the estuarine zone of

the eastern region, it was 1%.

4.4. Regional differences in carbonate chemistry

The ratio of TA to the dissolved inorganic carbon concentration (TA:C_T) is of particular interest

because it serves as an indicator of the relative abundance of carbonate species (e.g., HCO_3^- and

CO_3^{2-}) in seawater. According to Wang et al. (2013), for a specific temperature and pressure, the

CO_2 system parameters, such as the aragonite saturation state and pH value, are closely correlated

17

with this ratio, which has been widely used in studies of seawater carbonate chemistry (Zeebe and Wolf-Gladrow, 2001).

Differences in the seawater TA: C_T imply, for example, differences in buffer intensity, also called buffer capacity (Revelle factor). The buffer intensity of the seawater carbonate system is at a minimum when $CO_3^{2-} \sim CO_{2aq}$, where the TA and C_T concentrations are approximately equal (i.e., when TA: $C_T \approx 1$).

In **Figure 8** (corresponding to the NW region), water with a relatively low salinity (<35) dominates. A linear regression line derived from the SSS=20-37 portion of the TA-SSS plot produced a very low TA. In contrast, in **Figure 8C** (SW region), high SSS values (>32) are observed in the TA-SSS plot. This region is not affected by major river discharge. The variations in TA and SSS are assigned to physical factors, especially the balance between precipitation and evaporation.

The eastern edge (**Figure 8B** and **Figure 8D**) has regions with high productivity associated with the discharge of large rivers, such as the Niger and Congo Rivers. In **Figure 8B,** a very low TA was observed at zero salinity. As indicated in Section 3.5, low rates of CO_2 consumption have been reported for the Niger and Congo Rivers. As a result, the chemical, geological, biological and physical environments of coastal areas are affected. Low-salinity regions at the eastern edge (SSS <35) in the Atlantic Ocean can be found in two regions according to Bakker et al. (1999): one north of the equator and one near the Congo River. In contrast, in high-salinity offshore waters (>32), TA and SSS exhibited a tight linear correlation with an elevated TA.

The in-situ observations of TA and C_T obtained in the coastal regions of Africa and Brazil show significant differences (Bonou et al., 2016b). The biogeochemical composition of each border is different, and many different processes occur at each border, which are different from one another, including in the SSS≥35 regions.

18

Figure 8

The values observed here showed typical values for tropical waters, with a slight increase in the average values in the TA:CT (SW region; **Figure 9C**).

Figure 9B to **Figure 9D** show a relatively well-buffered TA: $C_T > 1.15$, while **Figure 9A** indicates a minor buffering capacity (TA:C_T =1.1). A lower buffer capacity may respond to coastal acidification, such as increases in atmospheric CO_2 or eutrophication events.

Biogeochemical processes such as photosynthesis, respiration (P-R), and air–sea CO_2 exchange also change the C_T. Changes in the C_T in regions with high fluvial discharge can alter these processes and consequently reduce the TA:C_T ratio. In the SW region, TA:C_T is high, making conditions more favorable for oceanic uptake of atmospheric CO_2.

Figure 9

5. Conclusions

The tropical Atlantic Ocean receives an important amount of carbon from the African and South American continents, which present different features at their oceanic borders. In this work, the comparative study of TA and C_T data from the coastal region of Africa and Brazil shows significant differences between these variables (Mann–Whitney test, $\alpha=0.05$, $p=0.0001$). These differences are explained by the differences in biological activities, the influence of rivers, and the composition of biogeochemicals in different coastal areas. At the western tropical border, the minimum values of the carbon parameters were obtained, while higher values of the carbon parameters were obtained in the eastern tropical Atlantic border. The biogeochemical composition of each border is different, and many different processes occur at each border. The coastal upwelling process at the

19

eastern border contributes to the higher CO_2 concentrations obtained in the eastern coastal area compared to those obtained at the western edge. This physical process increases the CO_2 parameters in surface water, followed by an additional physical process that transports the rich water masses from the African coast to the Brazilian coast through oceanic circulation (SEC). The river characteristics at each border are different in terms of their physical and biological activities and chemical composition. The existing TA and C_T relationships present spatial limitations, and the use of the empirical TA relationship determined by Lefèvre et al. (2010) for the observation data at the eastern border presents high root mean square error values. The similarity between the relationships from Takahashi et al. (2014) and Lefèvre et al. (2010) suggests that calculation of the carbon parameters in the eastern region, using one of these relationships, will lead to a higher root mean square error value. Otherwise, the climatological map determined by Takahaski et al. (2014) in the eastern region using this relationship may be affected by an important bias compared to that in other regions. On the other hand, the TA relationship determined by Koffi et al. (2010) is not a better relationship to be applied to the coastal data in the Amazon plume. However, we found that their relationship with TA can be extended to the southwestern part, mainly in the SEC region, for data with SSS≥37.

In coastal regions, the biogeochemical composition of each border is different, and many different processes occur at each border, principally regions that include values for SSS<35.

Author contributions

All authors contributed extensively to the interpretation of the results and to the writing of the manuscript.

20

Conflict of Interest Statement: The authors declare that the research was conducted in the absence of any commercial or financial relationships that could be construed as a potential conflict of interest.

List of figures

Figure 1. Routes of the different cruises (55 cruises), indicating the geographical positions of the total alkalinity (TA) samples in the Tropical Atlantic. The red and green colors represent samples collected from the western and eastern tropical Atlantic, respectively, with SSS<35, and the black points are data with SSS≥35 in the tropical Atlantic.

Figure 2. Standard deviation of SSS anomalies for the period from 1970-2013, showing the coastal regions with greater variability in SSS under the influence of rivers.

Figure 3. Monthly distribution of SST (°C) for January and July during the period of 1958-2014 in the tropical Atlantic.

Figure 4. SST climatology of the western and eastern regions for the 1958-2014 period (OAFlux database - http://oaflux.whoi.edu/). NW (-70°W to -35°W; 0° to 20°N); NE (-35°W to +10°W; 0° to 20°N); SW (-50°W to -15°W; 0° to -20°S); SE (-15°W to +10°W; 0° to -20°S).

Figure 5. Comparisons among **A**) empirical relationships of Koffi et al. (2010) and Lefèvre et al. (2010) for the estimated TA applied to data with SSS < 35 in the western tropical Atlantic; **B**) empirical relationships of Koffi et al. (2010) and Lefèvre et al. (2010) for the estimated TA applied to data with SSS < 35 in the eastern tropical Atlantic; **C**) empirical relationships of Koffi et al. (2010) and Lefèvre et al. (2010) for the estimated TA applied to data with SSS ≥ 35 in the central tropical Atlantic.

Figure 6. Localization of data with SSS≥37 around Koffi et al. (2010) lines in green and of data with SSS≥35 in black in the central region of the tropical Atlantic.

Figure 7. Annual average data from 10 years (2006-2015) of the chlorophyll-*a* concentrations in the tropical Atlantic Ocean (MODIS-Aqua; 4 km resolution), obtained from https://giovanni.gsfc.nasa.gov/giovanni/. (Data access: 2017.05.09).

22

Figure 8: TA-SSS relationship in the different subregions in the Atlantic Ocean.

Figure 9: TA:C_T for the NW region (A); NE region (B); SW region (C) and SE region (D). The black line TA:C_T =1; the dashed line indicates the tendency of the observed values. 4.7. C_T and TA normalization in the tropical Atlantic.

Figure 10: C_T bio ($C_{Texcess}$) derived from the mixing model in function SSS (a) in the western region and (b) in the eastern region

Tables

Table 1. Empirical carbon relationships available for the regions near tropical Atlantic Rivers.

REGION	EMPIRICAL RELATION	REFERENCE
Western	TA = 58 * SSS+265	Lefèvre et al. (2010)
	C_T = 50.1*SSS+0.9*(Year-1989) +198	Bonou et al. (2016a)
Eastern	TA = 65.52*SSS+2.50	Koffi et al. (2010)
	C_T = 51.71*SSS-12.79*SST +507.82	Koffi et al. (2010)
Tropical Atlantic	TA = 58.25*SSS+270.9	Takahashi et al. (2014a)

23

Table 2. Additional data cruises used in this paper with measurements of TA and C_T compiled with data from Bonou et al. (2016) for all tropical Atlantic Ocean data.

CRUISE	PERIOD	SHIP	REFERENCE	METHODOLOGY		PRECISION/ ACCURACY	
				TA[a]	C_T	TA (μmol kg^{-1})	C_T (μmol kg^{-1})
TTOTASSV	Dec 1982-Jan 1983	*R/V Knorr*	Takahashi et al.(2014b)	-	-	-	-
AJAX_1983	Oct 1983-Fev 1984	*R/V Knorr*	Chipman et al. (2007)	-	-	-	-
SAVE-1	Nov-1987	*R/V Knorr*	Takahashi et al. (1995)	-	-	-	-
SAVE-2	Dec-1987	*R/V Knorr*	Takahashi et al. (1995)	-	-	-	-
SAVE-3	Jan-1988	*R/V Knorr*	Takahashi et al. (1995)	-	-	-	-
WOCE-A16C (SAVE)	Mar-Apr 1989	*R/V Melville*	Takahashi et al. (1989)	-	-	±2/±2	±2/±2
CITHER 1	Jan- Mar 1993	*R/V Atalante*	Oudot et al. (1995)	-	Chromatography	-	-
EGEE-1	Jun-Jul 2005	*R/V Antea*	Koffi et al. (2010)	Full	-	±2/±2	±2/±2
EGEE-2	Sep 2005	*R/V Antea*	Koffi et al. (2010)	Full	-	-	-
EGEE-3	Mai-Sep 2006	*R/V Antea*	Koffi et al. (2010)	Full	-	-	-
EGEE-5	Jun-Jul 2007	*R/V Antea*	Koffi et al. (2010)	Full	-	-	-
EGEE-5	Jun-Jul 2007	*R/V Antea*	Koffi et al. (2010)	Full	-	-	-
EGGE-6	Set 2007	*R/V Antea*	Koffi et al. (2010)	Full	-	-	-
CITHER 2-1	Jan-Mar 1994	*R/V Maurice Ewing*	Rios et al. (2005)	-	SOMMA	±1.2/±1.2	±1.64/±1.6
WOCE-A15	Abr-May1994	*R/V Knorr*	Goyet et al. (1995)	Full	Colorimetry	-	-
METEOR 68/3	Jul-Aug 2006	*R/V Meteor*	Körtzinger & Steinhoff (2012)	Full	SOMMA	-	-
AMT7	Set-Oct 1998	*RRS James Clark Ross*	Lefèvre et al. (2002)	-	SOMMA	-	-
METEOR 80/1	Oct-Nov 2009	*R/V Meteor*	Körtzinger et al. (2012)	Full	SOMMA	-	-
FICARAM_XV	Mar-May 2013	*Hisperides*	Perez et al. (2013)	Full	-	-	-
CARINA.ATL	1999-2004	*Various ships*	This Study	Full	Potentiometry	-	-

[a]**Determined by potentiometric titration, either a full curve ("Full") or a single-point ("1-point") titration. No TA was measured during the AMT7 cruise.**

Table 3. Descriptive statistics (minimum as min, maximum as max, mean and standard deviation as STD) of TA and C_T in the eastern region (103 data points) and western region (392 data points).
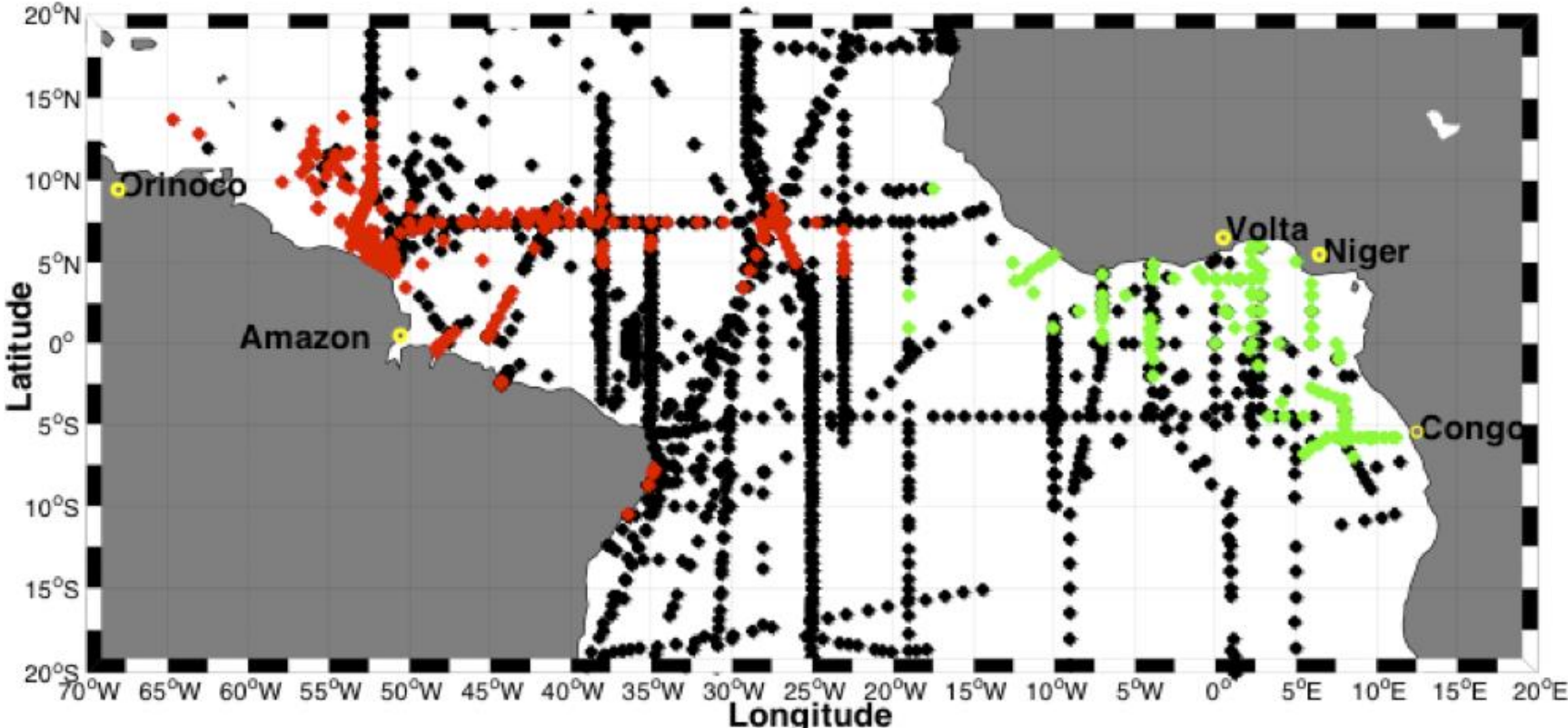
REGION	TA (μmol kg⁻¹)				C_T (μmol kg⁻¹)				SSS				SST(°C)			
	Min	Max	Mean	STD	Min	Max	Mean	STD	Max	Min	Mean	STD	Max	Min	Mean	STD
Western	323.0	2372.0	2099.4	286.4	397.7	2075.3	1779.6	236.4	34.9	1.1	31.	4.9	30.5	25.5	28.6	0.8
Eastern	1492.9	2320.7	2198.0	141.9	1389.6	2033.0	1892.2	94.2	34.9	22.9	33.6	2.1	29.1	22.8	27.8	1.2

Table 4. Root mean square error (rmse) of estimated TA and C_T from existing relationships.

PARAMETER	REGION	N	REFERENCE	RMSE (μmol kg⁻¹)
TA	Western (SSS<35)	392	Lefèvre et al. (2010)	28.6
			Koffi et al. (2010)	64.8
	Eastern (SSS<35)	103	Lefèvre et al. (2010)	28.5
			Koffi et al. (2010)	12.5
	Central (SSS≥35)	1848	Lefèvre et al. (2010)	20.5
			Koffi et al. (2010)	19.2
C_T	Western (SSS<35)	392	Bonou et al. (2016a)	41.1
			Koffi et al. (2010)	47.9
	Eastern (SSS<35)	103	Bonou et al. (2016a)	29.6
			Koffi et al. (2010)	28.1
	Central (SSS≥35)	1848	Bonou et al. (2016a)	35.1
			Koffi et al. (2010)	34,7

Figure 1

Figure 2

14
15
16
17
18
19
20 Figure 3
21
22
23
24
25
26
27
28
29
30
31
32
33
34
35
36
37
38
39
40 Figure 4
41

42
43
44
45
46
47
48
49
50
51
52
53
54
55
56
57
58
59
60
61
62
63
64
65
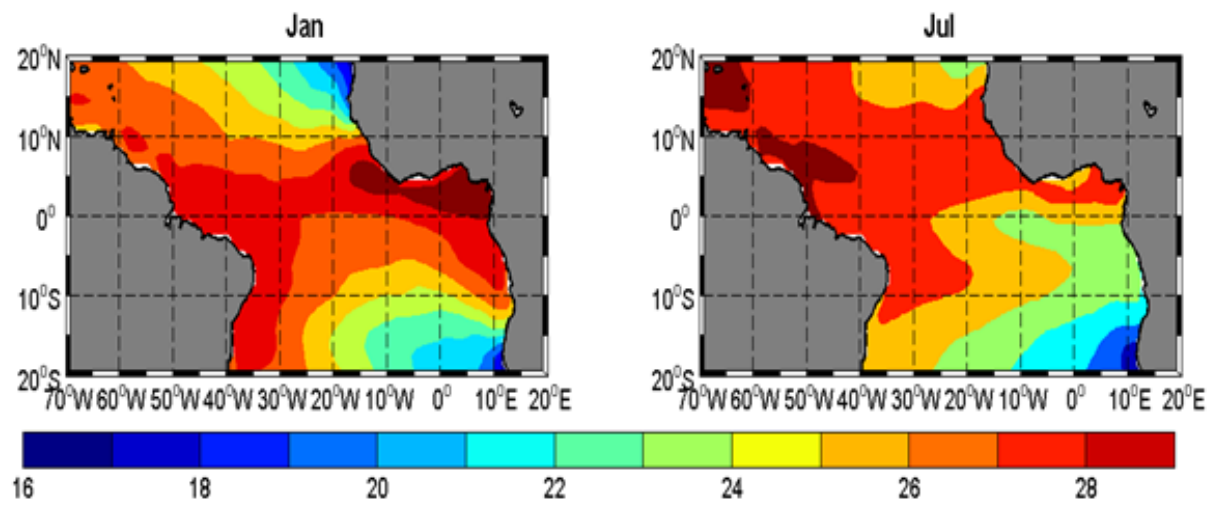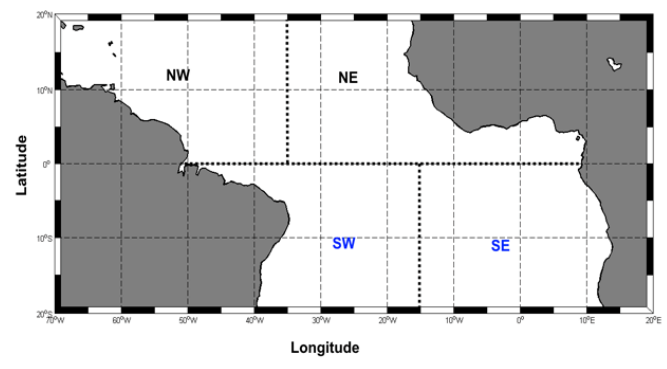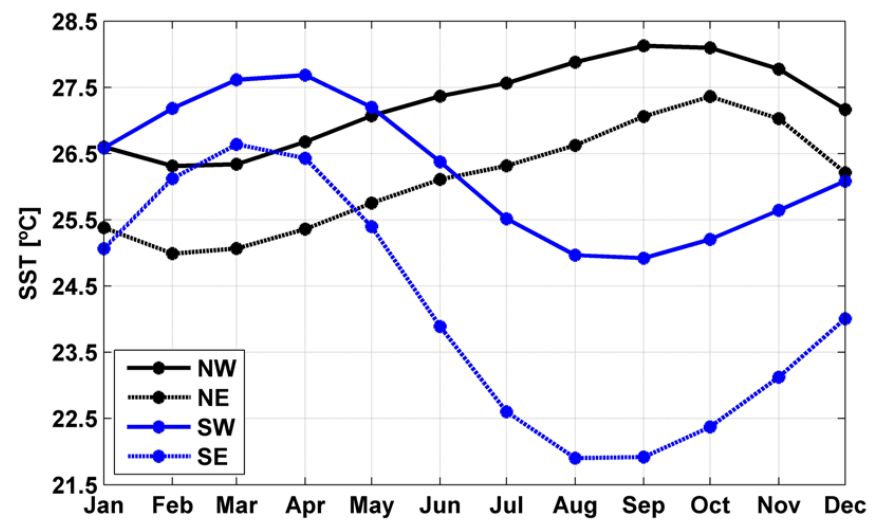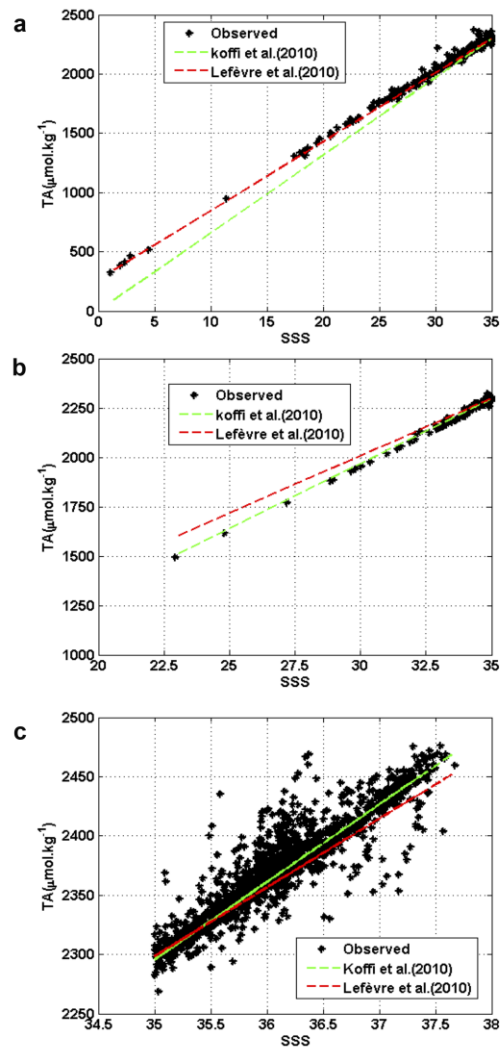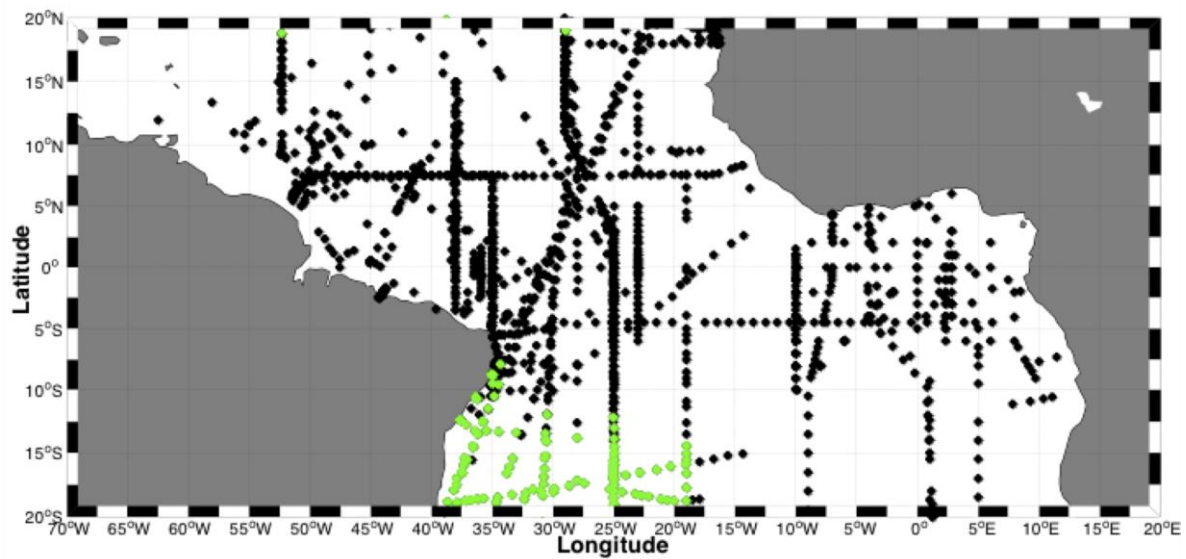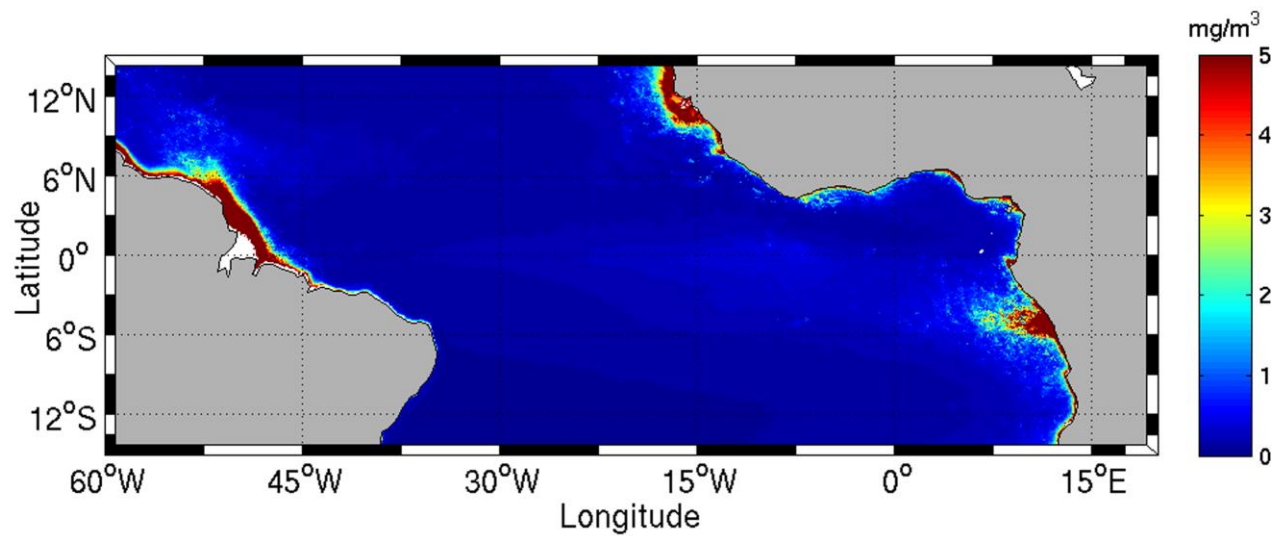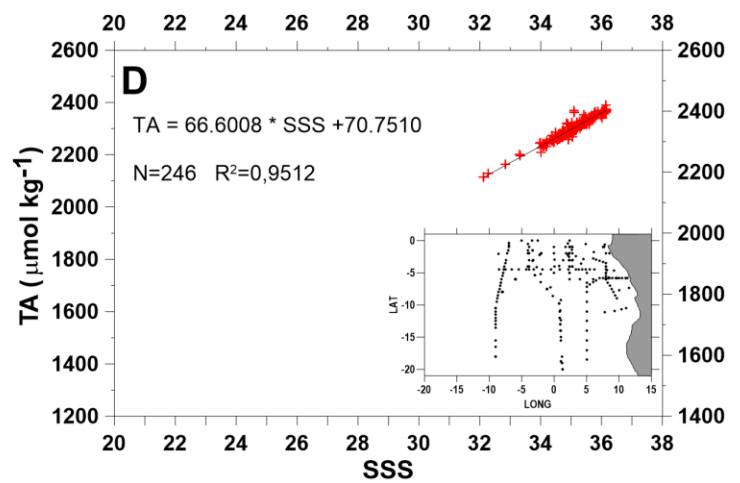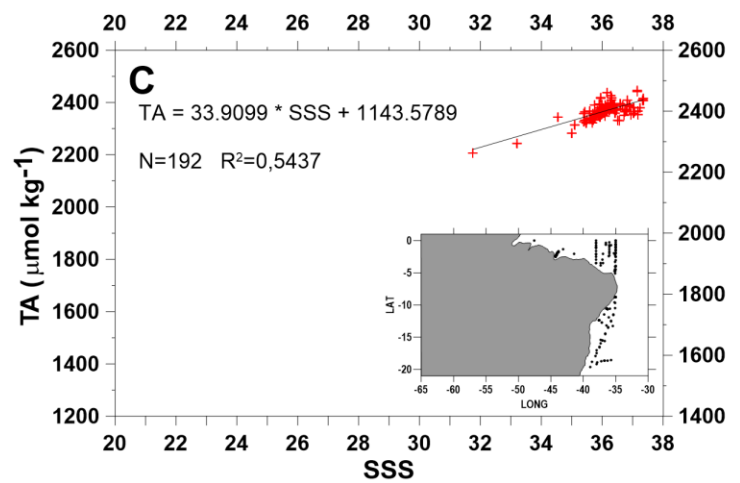
28

Figure 5

Figure 6

Figure 7

Figure 8

Figure 9

Figure 10

AJE®

Editing Certificate

This document certifies that the manuscript

A comparative study of total alkalinity and total inorganic carbon near tropical Atlantic coastal region

prepared by the authors

Frédéric Bonou, Carmen Medeiros, Carlos Noriega, Moacyr Araujo, Aubains Hounsou-Gbo and Nathalie Lefèvre

was edited for proper English language, grammar, punctuation, spelling, and overall style by one or more of the highly qualified native English speaking editors at AJE.

This certificate was issued on **May 26, 2022** and may be verified on the AJE website using the verification code **C1DE-BDD0-78A5-019D-89DC** .

Neither the research content nor the authors' intentions were altered in any way during the editing process. Documents receiving this certification should be English-ready for publication; however, the author has the ability to accept or reject our suggestions and changes. To verify the final AJE edited version, please visit our verification page at aje.com/certificate. If you have any questions or concerns about this edited document, please contact AJE at support@aje.com.

AJE provides a range of editing, translation, and manuscript services for researchers and publishers around the world. For more information about our company, services, and partner discounts, please visit aje.com.
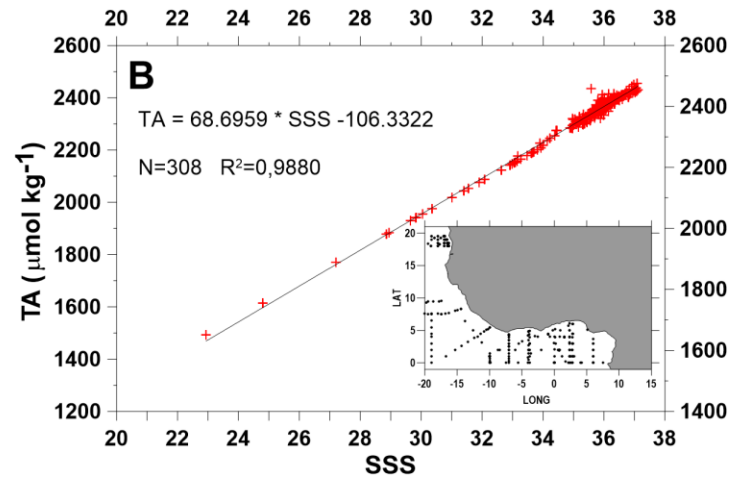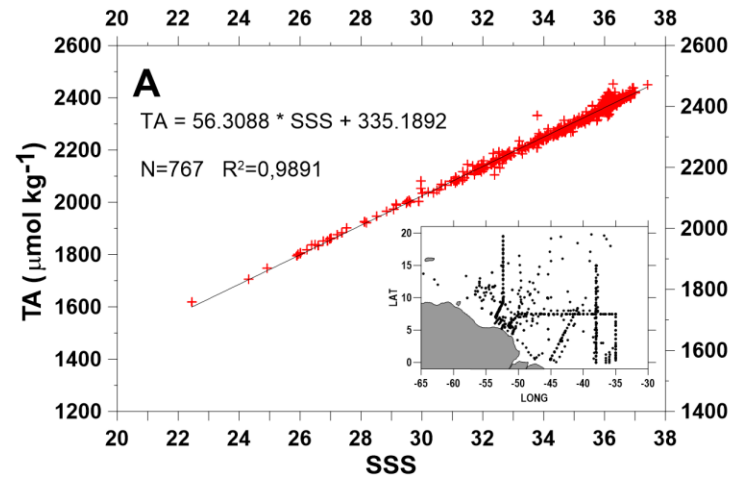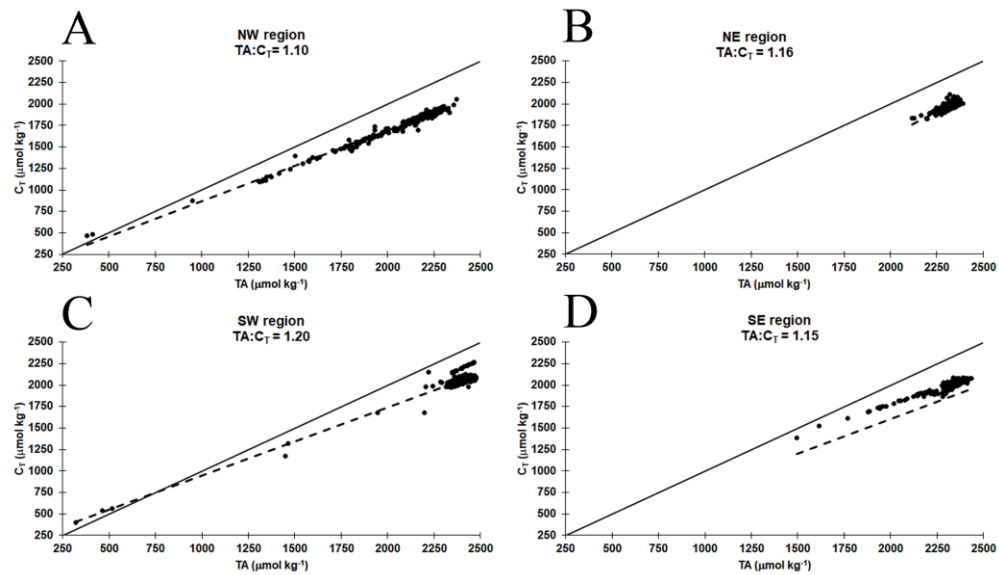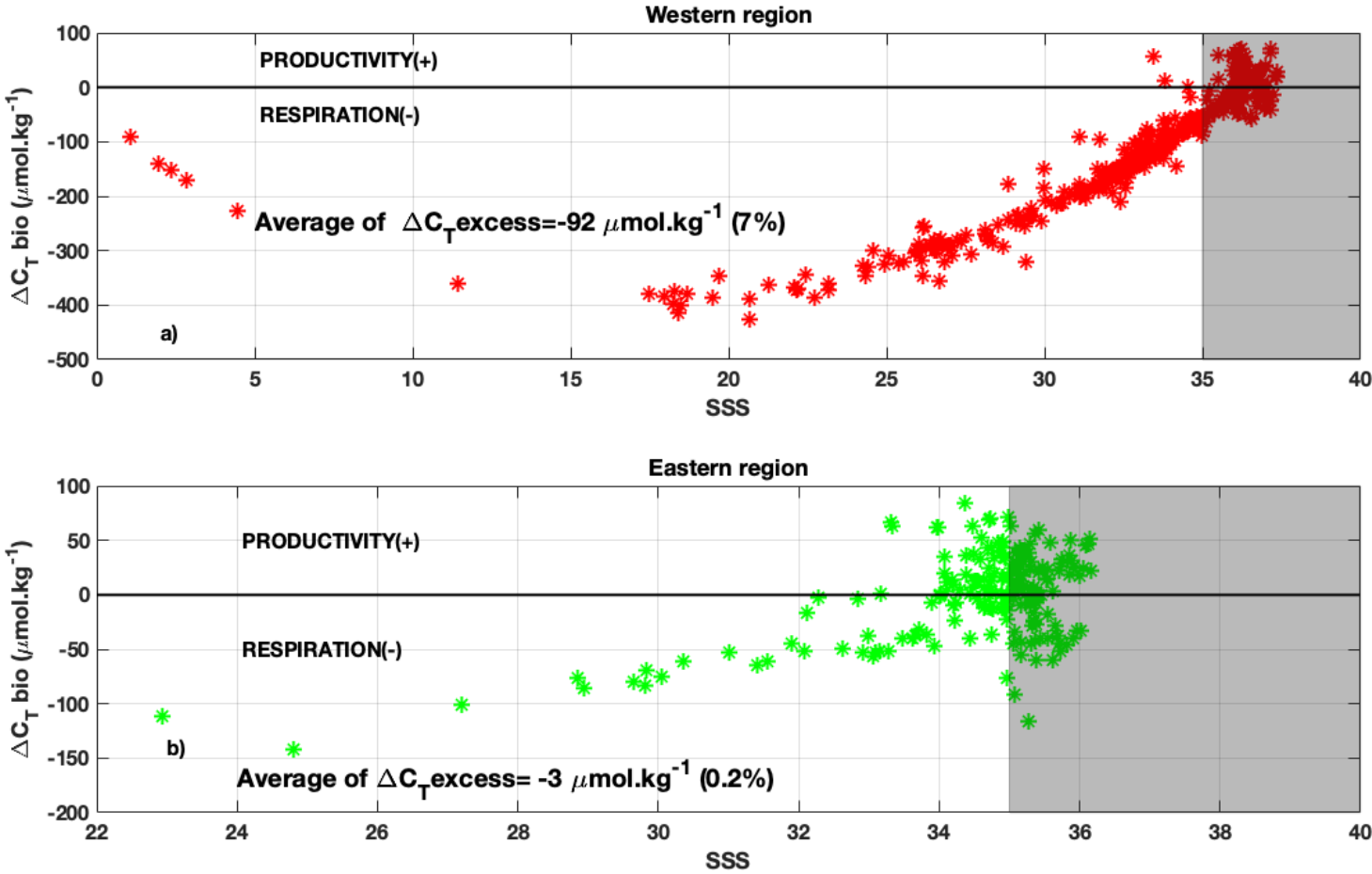
1
2
3
4
5
6
7
8
9
10
11
12
13
14
15
16
17
18
19
20
21
22
23
24
25
26
27
28
29
30
31
32
33
34
35
36
37
38
39
40
41
42
43
44
45
46
47
48
49
50
51
52
53
54
55
56
57
58
59
60
61
62
63
64
65

A comparative study ~~of~~ on total alkalinity and total inorganic carbon near the tropical Atlantic coastal region

> **Commented [A2]:** Your paper was edited for correct English language, grammar, punctuation, and phrasing. In addition, we have made some changes to ensure consistency throughout the paper. These changes are based on our extensive knowledge of what journals typically require. If you would like more details, please contact our Support team.

Abstract

This paper is based on a comparison of the carbon parameters at the western and eastern borders of the tropical Atlantic using data collected from 55 cruises. Oceanic and coastal data, mainly total alkalinity (TA), total dissolved inorganic carbon (C_T), sea surface salinity (SSS) and sea surface temperature (SST), were compiled from different sources. These data were subdivided into three subsets: oceanic data, coastal data and adjacent to the Brazilian (western) and African coastal areas (eastern) data. Significant differences between the TA data (2099.4±286.4 µmol kg^{-1}) at the western and eastern edges (2198±141.9 µmol kg^{-1}) were observed. Differences in the C_T values between the western edge (1779.6±236.4 µmol kg^{-1}) and eastern edge (1892.2±94.2 µmol kg^{-1}) were also noted. This pattern was due to the different variabilities ~~of~~in the carbon parameters between the eastern and western border coastal areas and to the biogeochemistry that drives these parameters. In the western coastal area, the physical features of the continental carbon and oceanic waters mixing ~~through~~ with the freshwater that flows from the Amazon and Orinoco Rivers to the South American coast are different than the physical features of the water that flows from the Congo, Volta and Niger Rivers in the eastern region. Applying the TA empirical relationship to TA with values of SSS<35 in the western and eastern ~~region~~regions leads to a higher root mean square error (rmse) in the eastern and western regions. Therefore, most of the existing TA empirical relationships are most useful at the regional scale due to the difference in the water properties of each region. The relationships of TA and C_T determined in the western and eastern regions do not reproduce ~~well~~ in-situ data well, especially at the adjacent edges. This difference is explained by the difference between the African and Brazilian coasts in terms of their carbon parameter characteristics and processes responsible ~~of~~for their variation. ~~Basing~~Based on the mixing model, it has been shown that the primary productivity in the eastern region is higher ~~when compared to that of~~ than that in the western region. This is one of ~~reason that makes~~ the reasons why the carbon parameters are higher in the eastern region. For each region studied, an equation for TA is introduced in this study.

1

Keywords: Carbonate system, Tropical Atlantic, West Africa, Brazilian border, Rivers, Coastal regions, Chemical oceanography.

Highlights

- ~~Compilation~~ Compiled ~~of~~ three decades of carbon data cruises.
- ~~Investigation~~ Investigated ~~of~~ TA/C_T differences in tropical Atlantic coastal zones.
- Significant difference between TA/C_T data from the African and Brazilian coastal areas were determined.
- High influence of C_T in the eastern region compared to that in the western region of the tropical Atlantic Ocean was recorded.
- Four empirical equations ~~are~~ were proposed for the four regions studied.

1. Introduction

~~From~~ Between the African and South American continents, the tropical Atlantic receives approximately 0.1 Pg C yr^{-1} of carbon, 0.046 Pg C yr^{-1} of dissolved organic carbon (DOC), and 0.053 Pg C yr^{-1} of dissolved inorganic carbon total (C_T) (Huang et al., 2012). According to Araujo et al. (2014), 13.2% of the C_T and 27.3% of the DOC global values are transported from rivers into the world's oceans. Furthermore, rivers provide 0.8-1.33 Pg C to oceans worldwide, of which ~ 0.53 Pg C is transported from tropical rivers (30°N- 30°S) to adjacent estuarine-coastal systems (Huang et al., 2012).

In the tropical Atlantic, the Amazon River is the ~~first~~ largest ~~major~~ river, flowing from west to east, while the Congo River is the second largest ~~major~~ river, which has a local dynamic in this area (Cai et al., 2008). The ~~transports~~ transport of terrestrial, oceanic and atmospheric carbon in the global carbon cycle ~~are~~ is influenced by rivers. ~~Freshwaters are~~ Freshwater is generally rich in terrestrial and atmospheric carbon and is transported to the ocean through rivers (Araujo et al., 2014). The high nutrient concentrations transported by the river flux within the continental shelf and adjacent

2

oceanic region increase primary production and can lead to the absorption of CO_2 (Körtzinger, 2003; Regnier et al., 2013). Previous studies have also revealed that South American estuaries (western region) and African estuaries (eastern region) are carbon sources (+10.6±7 mmoles m^{-2} day^{-1} and +7.0 mmoles m^{-2} day^{-1}, respectively) for the tropical Atlantic (Araujo et al., 2014). Therefore, the coastal regions adjacent to ~~the~~ rivers are regions with highly variable CO_2 parameters due to the carbon input that occurs through the discharge of rivers into ~~the~~ oceanic regions. The amount of carbon from the continental input at the ~~different~~ separate edges (eastern and western) can influence the carbonate system, such as the total alkalinity (TA) and total dissolved inorganic carbon (C_T). It is necessary to collect data at these edges to better understand the variability of these parameters.

Important processes can be responsible for carbonate chemistry changes in the ocean, and they can be described by considering the changes in C_T and TA. The invasion of CO_2 from (or the release of CO_2 to) the atmosphere increases (or decreases) C_T while TA remains constant, leading to a rise and drop of [CO_2], respectively, with opposite changes in pH (since CO_2 is a weak acid). Respiration and photosynthesis ~~lead~~led to the same trends, except that TA ~~changes~~changed slightly due to nutrient release and uptake. $CaCO_3$ precipitation decreases C_T and TA at a ratio of 1:2 and, counterintuitively, increases [CO_2], although inorganic carbon is reduced.

The spatial distribution of CO_2 and C_T in the surface ocean is mainly explained by the temperature-dependent solubility of CO_2 on interannual timescales. Because of increased solubility at low temperatures, warm low-latitude surface water retains less $C0_2$ (~10 μmol kg^{-1}) and C_T (~2000 μmol kg^{-1}) than cold high-latitude surface water (CO_2 ~ 15 mol kg^{-1} and C_T ~ 2100 mol kg^{-1}). Significant deviations from these broad trends may occur locally and on seasonal time scales due to changes in salinity and processes such as biological activity, upwelling, temperature variations, river runoff, and other activities that alter C_T and TA.

3

Some equations have been developed in recent decades to determine the carbon parameters TA, C_T and fugacity (fCO_2) as functions of physical and other parameters that are easily measurable and accessible (Takahashi et al., 2014, Lefèvre et al., 2010, Koffi et al., 2010). Linear regression relationships can be a good option to estimate carbon parameters. Empirical equations also present large uncertainties in data due to the complexity of the carbon parameters in coastal areas. Although empirical equations are useful to reproduce carbon parameters, they have spatial and temporal limitations for reproducing carbon parameters well in a whole oceanic basin. There have been few studies that focus ~~in~~on the tropical Atlantic with an emphasis on the contribution of river discharge to carbon. In 2006, other authors used the relationship TA vs. ~~vs~~ SSS (~~Sea Surface Salinity~~sea surface salinity) and SST (~~Sea Surface Temperature~~sea surface temperature) in the tropical Atlantic (30°S-~~30ºN~~30°N) for oceanic regions with the SSS criterion ~~of SSS~~ (greater than 31) (Lee et al., 2006). This empirical relationship cannot be used for data with low SSS in these regions with higher discharge due to major rivers. In the tropical Atlantic, Takahashi et al. (2014a) determined and used only one empirical relationship of TA regression for the whole tropical Atlantic basin; this relationship is similar to the one determined by Lefèvre et al. (2010), specifically for the Amazon region. In the same year, Koffi et al. (2010) determined a different TA relationship in the eastern Gulf of Guinea, with a slope that was highly different from that determined in Lefèvre et al. (2010) and Takahashi et al. (2014a). Due to the spatiotemporal variability, in the western region, an empirical relationship of C_T was obtained by Bonou et al. (2016a) using SSS and time variation (year), while in the eastern region, Koffi et al. (2010) determined an empirical relationship of C_T using SST and SSS (**Table 1**). It is desirable to continue studying the performance of linear regression, multiple regression or other methods to obtain a better estimation of the carbon parameters. The compilation of many data cruises, within the context of acquiring new observation

4

data, is a good means to determine existing relationships in order to have robust equations that are adaptable to the regions, leading to smaller uncertainties.

Table 1

Data from different sources are compiled from different oceanographic data cruises (1983-2014) to compare the TA and C_T variations in the western and eastern tropical Atlantic, mainly in coastal areas adjacent to rivers. The compilation of several data cruises was used to test the reliability of the existing relationships and to reproduce the TA/C_T distribution in these transition regions. A comparative study was ~~done~~performed to emphasize the limits and differences in the variation ~~of~~in TA/C_T at the tropical Atlantic borders.

2. Material and Methods

2.1. Database and methodology

 All available cruise data were extracted from oceanographic and voluntary merchant ships (20°S-20°N, 70°W-15°E) in the tropical Atlantic ~~that~~, which is the study area where in situ data TA, C_T, SST and SSS were sampled and measured (**Figure 1**). In Figure 1, the data are shown in red and green for SSS<35 (points in black ~~color~~ indicate SSS>35). The dataset was acquired from 1983 to 2014 through 55 campaigns (**Table 2**) completed with those used in Bonou et_al. ~~Al~~ (2016). Conductivity, temperature and depth data acquired with CTD and bottle samples during those surveys were obtained from the Carbon Dioxide Information and Analysis Center (http://cdiac.ornl.gov/oceans/bottle_discrete.html).

Figure 1 (Single Column)

5

Table 2

The TA and C_T data used in this study were obtained from data cruises, and were determined by potentiometric titration from either a full curve ("Full") or a single-point ("1-point") titration. The SSS database was obtained from an updated version of SSS data from 2013 by Reverdin et al. (2007). These data were used as indicators for determination of the area affected by freshwater due to rivers in the tropical Atlantic. The monthly SST data were extracted from the Objectively Analyzed air-sea Fluxes Project (OAFlux) database (with $1°$ of longitude and $1°$ of latitude). The SST data used in this study were acquired from 1958-2014, and the data are available on the Woods Hole Oceanographic Institution (WHOI) website at oaflux.whoi.edu. The OAFlux project provides a synthesized product generated from the reanalysis datasets NCEP1, NCEP2, ERA40 and ERA (Yu and Weller, 2007, Yu et al., 2008).

The TA and C_T relationships used were determined by different authors (see **Table 1**) to verify their limits to reproduce data compared to the observation data, especially at the eastern and western borders.

2.2. Statistical analysis

Statistical analysis and the Mann–WhitneyMann Whitney test were used to compare two sets of data (TA, C_T, SST, and SSS) from different areas (western tropical Atlantic and eastern tropical Atlantic) to determine the difference between the carbon parameters (TA and C_T) in the different localities. Linear regression methods were applied to determine and test the connections between the physical parameters and carbon parameters; this method was also used to observe the best fit

6

that matched the observation data. To compare these different relationships, the root mean square

error (rmse) was calculated as follows:

$$\text{rmse} = \left[\frac{1}{n\text{-}1} \times \sum_{i=1}^{n} \left(X_i \text{-} Y_i \right)^2 \right]^{\frac{1}{2}} \quad (3);$$

where Xi is the observed value and Yi is the modeled value at time/place i.

The Kruskal–WallisKruskal Wallis test was used to identify significant differences (α=0.05)

between all regions. Additionally, Dunn's test was applied to identify significant differences

between borders (NW, NE, SW, and SE, for α=0.05) and between hemispheres.

3. Results

3.1. The distribution of SSS and SST anomalies in the tropical Atlantic

Standard deviations of SSS anomalies computed for the period from 1970-2013 using the database

from Reverdin et al. (2007) actualized in 2013, allowed us to map the areas under distinct degrees

of influence of freshwater input due to river discharge and/or precipitation (Figure 2). The regions

presenting high SSS variability (SD>1) along the South AmericanAmerica corresponded to coastal

areas adjacent to the mouthmouths of the Amazon and Orinoco riversRivers and areas along the

African coastal border adjacent to the Congo, Niger and Volta riverRiver mouths. Lower

variations in SSS anomalies were observed in the oceanic zone and along coastal areas not

receiving large river discharge, as is the case offor the NE-Brazilian coast and the northern coast

of Africa. The São Francisco riverRiver in NE- Brazil (**Figure 2**) does not induce significant

variation in the SSS due to the presence of numerous dams of hydroelectric plantplants along its

course, drastically reducing drastically its flow despite the extension of its drainage basin.

Figure 2 (Single Column)

7

The SST distribution in the study area presents a seasonal zonal pattern with less variable values along the western Atlantic relative to that of the eastern Atlantic. SST along the South American coast varies from 26 to ~~28°C~~28 °C~~8°C~~ in January and between 25 and ~~29 °C~~29 °C~~9°C~~ in July. Along the African coast, SST is higher (~~>27°C~~>27 °C~~7°C~~) in the eastern Atlantic (~~0°~~0° to ~~5°N~~5°N) in January, and lower (~~<26°C~~<26 °C~~6°C~~) ~~on~~in coastal areas between the equator and ~~10°S~~10°S in July (**Figure 3**).

Figure 3 (Single Column)

The annual amplitude of the SST in the western Atlantic (including 20°°S-20°°N; 70°°W-30°°W) was 3.0 °C~~0°C~~. However, in the eastern Atlantic (including 20°°S-20°°N; 20°°W-15°°E), the amplitude of the SST was 5.7 °C~~7°C~~ (**Figure 3,4**).

Figure 4 (1.5 Column)

A subset division of the tropical Atlantic Ocean into four regions (NW, SW, NE and SE) is included according to the variability in the SST climatological. This division sought to differentiate the variations between the hemispheres and the continental borders (**Figure 4**).

The Kruskal–Wallis~~Kruskal Wallis~~ test showed significant differences (α=0.05; p=0.0007) between all regions. Additionally, Dunn's test showed significant differences between borders (NW $\neq$ NE; α=0.05; p=0.012 and SW $\neq$ SE; α=0.05; p=0.008) and between hemispheres (NW $\neq$ SW; α=0.05; p=0.009 and NE $\neq$ SE; α=0.05; p=0.003).

8

For SSS<35 (freshwater influence), the statistical test also confirmed a significant difference between the SST values of the eastern and western regions (Mann–WhitneyMann Whitney test, p=0.0001; α = 0.05).

3.2. TA and C_T in the tropical Atlantic

Three hundred ninety-two in situ coastal data samples of TA, C_T, SSS and SST from the western region, represented in red, were used in this study and compared to 103 data samples of TA, C_T, SSS and SST from the eastern region, represented in green (**Figure 1**). All these data were obtained under the criterion of SSS being less than 35 psu. A significant difference was observed when the selected TA and C_T data (in red points) from the western Atlantic were compared with TA and C_T data (green points) from the eastern tropical Atlantic. At the western edge, the average value of TA (2099.4 ± 286.4 µmol kg^{-1}) was obtained; this value was lower than the value obtained from the eastern tropical Atlantic (2198 ± 141.9 µmol kg^{-1}) (**Table 3**), while the standard deviation indicated a higher variation in TA in the western region than that obtained in the eastern region (Mann–WhitneyMann Whitney test, $p = 0.0008$, α = 0.05). For the C_T variable, (1892.2 ± 94.2 µmol kg^{-1}) and (1779.6 ± 236.4) µmol kg^{-1} are the mean values and the standard deviation obtained, respectively, at the eastern and western borders.— The standard deviation on CT in the western border iswas higher than that of the eastern border, it is showing that higher variation ofin TA and CT thein South America than in the African border (Mann–WhitneyMann Whitney test, $p = 0.00002$, α = 0.05).

Table 3

9

This result supports the higher average values of TA and C_T (**Table 3**) in the eastern region Koffi et al. (2010) and the higher TA and CT values in the Gulf of Guinea, especially in this upwelling region (**Figure 4**).

3.3. Relevance and limitation of existing relations for TA and C_T in the tropical Atlantic.

The relationships proposed by Lefèvre et al. (2010), Koffi et al. (2010) and Bonou et al. (2016a) (**Table 4**) were used to compute TA and C_T and to observe their spatial relevance and limitations in the tropical Atlantic. The data in red and green samples have SSS ~~is~~values lower than 35, while the data in black correspond to ~~that~~those of the regions where SSS is higher than 35 (**Figure 1**).

Table 4

Observations of SSS<35 in the western border are due to the higher influence of rivers and freshwater due to the retroflexion of Amazonian waters by the North Brazilian Current (NBC) and into the NECC, which is beyond the influence of rainfall in the equatorial region due to the ITCZ (~~InterTropical Convergence Zone)~~ intertropical convergence zone). In this region, the empirical relationship proposed by Lefèvre et al. (2010) represents the TA observations better than the relationships proposed by Koffi et al. (2010) (**Figure 5A**). The standard deviation of TA from Lefèvre et al. (2010) was 28.6 µmol.kg^{-1}, while that obtained for TA by Koffi et al. (2010) was 64.8 µmol.kg^{-1} (**Table 4**). The greatest discrepancies occur for data with SSS<30.

Figure 5 (Single Column)

The opposite trend was observed in the eastern region, where the relationship described in Koffi et al. (2010) is better at reproducing the observation data than that described in Lefèvre et al.

10

(2010) (**Figure 6**). The rmse value of TA was 12.5 μmol kg^{-1}, which was obtained from the relationship from Koffi et al. (2010) in the eastern region. This rmse value TA is almost two times lower than that obtained with the relationship of Lefèvre et al. (2010) (**Table 4**). This result ~~is in agreement~~agrees with that obtained in Lefèvre et al. (2010), which showed the best fit of TA with SSS when using Koffi et al. (2010).

Figure 6 (1.5 Column)

3.4. Biological processes

In the western and eastern tropical Atlantic, biological consumption is one of the processes that ~~influence~~influences the variation ~~of~~in the carbon parameters around ~~the~~ tropical edges (Cooley et al., 2007; da Cunha et al., 2013; Araujo et al., 2014).

As explained above, the surface C_T concentration is influenced by lateral and vertical mixing of water with different levels of C_T (the transport effect), photosynthesis and oxidation of organic matter (the biological effect) and changes in temperature and salinity (Takahashi et al., 1993; Lee et al., 2000). However, these effects are ~~direct~~directly or indirectly correlated with SST, but the trends often differ seasonally and geographically.

According to Koffi et al. (2010), equatorial upwelling and coastal upwelling along the eastern boundary merge to form a cold tongue during the main upwelling season, and the cold tongue undergoes advection westward by the South Equatorial Current (SEC). This cold tongue transports CO_2-rich waters, and fCO_2 increases as the surface water temperature increases toward the west. The Guinea Current (GC) and ~~(~~SEC~~)~~ are influenced by several fluvial contributions, including the Volta River (4°N-0°), Niger River (3°N, 8°E) and Congo River (-6°S, 12°E) (Koffi et al., 2010).

11

The eastern border is strongly affected by biological activity (NE and SE). The average C_T was 2056 μmol kg^{-1}, which is close to that of the Atlantic Ocean, as indicated by Millero (2006).

The satellite data through the MODIS-Aqua sensor were used ~~to~~for the study region. The highest concentrations of chlorophyll-*a* are observed in the coastal regions near the Amazon River, Orinoco River, Congo River and NW ~~of~~ Africa (coastal upwelling) (**Figure 7**).

4. Discussion

4.1. Analysis of the regions influenced by tropical Atlantic Rivers

The ~~distribution of the~~ standard deviation distribution of anomalies was used by Bonou et al. (2016a) to identify regions with higher variations ~~of~~in the variables considered. In our work, this method was applied to investigate the ~~sub regions~~ subregions of the tropical Atlantic characterized by higher variations in SSS (**Figure 2**). The fact that almost all the regions of the tropical Atlantic presenting large ~~SD~~SDs of SSS anomalies were located near tropical rivers presenting high discharge corroborates that this method is robust to ~~identify~~identifying the influence of its discharge on salinity.

The standard deviation of SSS was an anomaly with values between 0.2 and 2.0 for the coastal regions of the study area. There is a significant difference between the SSS anomalies (Mann–Whitney~~Mann Whitney~~ test, p=0.0005; $\alpha = 0.05$) at the western and eastern borders of the tropical Atlantic. The hydric balance of the Amazon and Orinoco Rivers at the western edge is greater than the balance of the Congo, Niger and Volta Rivers at the eastern border (Dai and Trenberth, 2002; Cai et al., 2008; da Cunha et al., 2013; Araujo et al., 2014). According to Bonou et al. (2016a), in the tropical Atlantic, the variation in SSS is higher in the western region, with SSS values between 1 and 38.

12

The western tropical Atlantic shows a higher variability in SSS and a less pronounced seasonal variability in SST. On the other hand, the eastern tropical Atlantic presents a lower variability in SSS but a strong seasonal variability in SST (**Figures 2, 3 and 4**). This area ~~experiencing~~experiences coastal upwelling (Schneider et al., 1997; Dale et al., 2002) ~~were~~, where a rise ~~of~~in cold-water masses rich in nutrients and CO_2 is observed and ~~where~~ surface coastal water is pushed ~~off-shore~~offshore by Ekman divergence.

The SSS is a physical parameter that has a high correlation with carbon parameters, and its variability is believed to impact carbon parameters. In the Tropical Atlantic, the SSS is highly correlated with TA and CT (Bonou et al. (2016a), Koffi et al. (2010), Lefèvre et al. (2010); therefore, the stronger influence of the Amazon and Orinoco Rivers in the western tropical Atlantic is one explanation for the difference observed in the carbon parameters between the eastern and western regions.

4.2. Pertinence of existing relations to the tropical Atlantic.

The results presented in **Figures 5A** and **5B** show that the relationships from Lefèvre et al. (2016) are adapted in the western tropical Atlantic region mainly in the Amazon and Orinoco Rivers, while the relationship from Koffi et al. (2010) reproduces the observations in the eastern tropical Atlantic well, mainly in the Gulf of Guinea.

In the central basin of the tropical Atlantic, the results with SSS≥35 showed that the behavior was very close between the two empirical relationships (**Figure 5C**). The relationship from Lefèvre et al. (2016) had a slightly higher rmse value than that obtained from the relationship from Koffi et al. (2010) (20.5 and 19.2 μmol kg^{-1}, respectively). According to these results, the use of the two empirical relationships yielded similar TA values in the central region when SSS≥35 psu.

13

Almost all TA data with SSS≥37 are clustered around the green line, which is the line represented

by the relationships from Koffi et al. (2010). Data with SSS≥37 are located in the ~~SEC~~ region ~~of~~

~~the SEC~~ (**Figure 6**), which ~~is extended~~ extends to the western part. This result means that the

relationship from Koffi et al. (2010), as determined in the eastern region, can be extended into the

western part of the SEC.

Analysis of the proposed relationships ~~proposed~~ used to determine C_T is more complicated, at least

regarding its graphical representation. In the eastern region, Koffi et al. (2010) determined C_T

relationships using SSS and SST, while Bonou et al. (2016a) determined a C_T relationship using

only the SSS function but still considered its temporal variation (**Table 3**) in the western tropical

Atlantic region. The C_T relationships in both regions (western and eastern) do not depend only on

SSS and TA relationships. In this case, C_T cannot be estimated only as a function of a single SSS

parameter, and the statistical results are presented in **Table 4**~~,~~ (Bonou et al., 2016b).

In the western tropical Atlantic, the rmse value was obtained from the estimated C_T derived from

Bonou et al. (2016a), and this value was 41.1 µmol kg^{-1} considering that the relationship from Koffi

et al. (2010) gives 47.9 µmol kg^{-1} as the rmse value. In the eastern region, the rmse value obtained

from the estimated C_T relationship from Koffi et al. (2010) was 28.11 µmol kg^{-1}, while from Bonou

et al. (2016a), the rmse value was 29.6 µmol kg^{-1}. In the oceanic region (SSS≥ 35), the rmse values

were also similar between the two empirical relationships (34.7 and 35.1 µmol kg^{-1} for Koffi et al.

(2010) and Bonou et al. (2016a), respectively). In fact, the greatest variation in SST observed in

the eastern edge of the basin contributes to the C_T equation since SST is one of the key state

variables that influence the carbon cycle in this region (Lefèvre et al., 2008; Koffi et al., 2010,

Bonou et al., 2016b). On the other hand, the empirical relationships of C_T proposed for the western

edge do not ~~take into account~~consider SST because their variation is lower at the western edge than

14

in the eastern region (Lefèvre et al., 2010; Ibánhez et al., 2015; Bonou et al., 2016a). According to Key et al. (2004), the surface C_T distribution is affected by physical processes; however, the pattern is more similar to that of nutrients (e.g., nitrate) than to that of salinity. This is because C_T concentrations are more strongly affected by biology than ~~those of TA~~TA concentrations.

4.3. Lithological composition of basins and influence of plumes

The different rock types that dominate the river basins influence the input of CO_2 through rock weathering and through riverine transport of inorganic carbon to the ocean. The chemical erosion of inorganic materials consists of dissolving or hydrolyzing primary minerals of rocks and soils. The chemical reactions require CO_2 and release C_T (mainly as HCO_3^-). Thus, different rock types have different CO_2 consumption rates. According to Amiotte-Suchet et al. (2003), high CO_2 consumption rates are observed in carbonate rocks, moderate CO_2 consumption rates are observed in basalts plus shales, and low CO_2 consumption rates are observed in shales plus and sands/sandstones. Thus, the Amazon and Orinoco Rivers have high CO_2 consumption rates, and the Congo and Niger Rivers have moderate and low CO_2 consumption rates. Araujo et al. (2014) observed that the contribution of the mean CO_2 fluxes consumed by the total HCO_3^- ~~rivers~~river flux was 82 and 88% for the western border and eastern border, respectively. These authors also indicated that during a dry period, the atmospheric CO_2 flux consumed through rock weathering was lower than that during a more humid period. However, middle-latitude and subtropical larger rivers have high bicarbonate (HCO_3^-) concentrations and fluxes because of the abundant distribution of carbonate minerals in their drainage basins. In contrast, tropical larger rivers ~~have low HCO_3^- concentrations~~, such as the Amazon and Orinoco Rivers~~,~~ have low HCO_3^- concentrations (Cai et al., 2010).

15

Large rivers also generate offshore plumes that are characterized by high buoyancy and biological productivity because of their low salinities, high levels of nutrients, and suspended and dissolved terrestrial materials (Higgins et al., 2006; Kouamé et al., 2009; Kang et al., 2013). As a result, the chemical, geological, biological and physical environments of the adjacent marginal seas are affected. Low-salinity regions at the eastern edge (SSS <35) in the Atlantic Ocean can be found in two regions according to Bakker et al. (1999): one north of the equator and one near the Congo River. Van Bennekom et al. (1978) and Vangriesheim et al. (2009) showed that the influence of the Congo River ranges from -3.5° to -6.5° latitude and reaches 6.5° E in the Atlantic Ocean (700 km offshore).

In the Atlantic Ocean, the dispersal of the Amazon River water leads to a brackish water plume that can exceed 10^6 km^2, reaching latitudes as far from the river mouth as 30°W (Coles et al., 2013) or even 25°W when the North Equatorial Countercurrent (NECC) is strong (Lefèvre et al., 1998). Recently, Ibánhez et al. (2017) compared the monthly precipitation rate with the monthly SSS in five regions of the tropical Atlantic. They found highly significant linear relationships of precipitation with SSS across the western Atlantic basin. The extension of the Amazon River plume was highly significant, ranging from 0.25 to 1.60×10^6 km^2, after removing the influence of rainfall. In Tropical Atlantic regions, low salinity patches are related to large rivers, such as the Amazon (5413 km^3 year^{-1}), followed by the Congo (1263 km^3 year^{-1}) and Orinoco (1170 km^3 year^{-1}), spreading freshwater by surface oceanic circulation (Araujo et al. 2014).

According to (Araujo et al. (2014), significant differences were observed between the large estuarine systems of the Atlantic Ocean. The authors indicated that C_T and TA showed significant differences between the eastern (Volta, Niger and Congo Rivers) and western (Orinoco, Amazon, São Francisco and Paraíba do Sul riversRivers) estuaries. Other important parameters also showed significant differences, such as pCO$_2$ and dissolved organic carbon (DOC). According to these

16

authors, DOC is higher in the eastern region; this would affect coastal concentrations in that region, increasing C_T levels in the adjacent coastal region. Additionally, TA is mainly affected by the chemical reactions of the different types of rocks in the soils of the hydrographic basins, which are carried to the coastal region via runoff

~~Basing~~Based on the approaches of Ternon et al. (2000), Körtzinger (2003), Cooley and Yager (2006) and Araujo et al. (2014), a simple conservative mixing model ~~has been~~ was used to calculate the proportions of C_T in western rivers (Amazon and Orinoco) and eastern rivers (Niger, Volta and Congo) for ~~the~~ plume water and seawater in a given plume sample (Figure 10). This ~~approach of~~ mixing model approach has been widely detailed in the supplementary material of Araujo et al. (2014). ~~it~~It is assumed that the effects of precipitation and evaporation on the carbon and freshwater mass balances are small compared to the river (Cooley and Yager, 2006) over the first 10 m-deep plume. Additional variations in CT not attributable to mixing were then ascribed to biology (CTbio). Using the mixing equations of Araujo et al. (2014), we used TA, SSS and CT to estimate the excess or deficit of CTbio in the east and west coastal regions (TAbio calculation is not necessary here, as TA is considered ~~as~~a conservative parameter). Positive values of ΔCTbio indicate an inorganic carbon deficit, implying that the respiration process exceeds the respiration process. Thus, the system is considered to be autotrophic~~;~~, while negative CT values indicate excess CT, suggesting that respiration > production, and the system is considered heterotrophic. The results showed that~~:~~ both regions ~~have~~had negative CTbio values in the estuarine region, indicative of excess CT. Outside the plume, the values oscillate between positive and negative; however, the mean values of the gradients indicate excess CT. In the western region, 7% of the CT excess (bio) average across the entire saline gradient ~~has been~~was obtained, while in the eastern region, this percentage was lower (0.2%). According to these results, ~~it considered that~~the primary productivity in the eastern region is higher ~~when compared to that of~~than that in the western region

17

(~~Figure10~~Figure 10 a and b). Additionally, we have to consider that the extension of the plumes differs, and the saline values are smaller in the western region, generating a greater amplitude of variation between the CT values. The concentrations of HCO_3^- (the main component of CT coming from the rocks) in the eastern region are higher; however, the freshwater flow is greater in the western region. The observed concentrations showed that~~:~~ the western region has an average CTbio excess of 92 ~~umol~~μmol kg^{-1}, while the eastern region has an average CTbio excess of 3 ~~umol~~μmol kg^{-1}. In estuarine zones, these excesses of CT are greater. In the western region, ~~can reach~~it reached 14%, while in the estuarine zone of the eastern region, it was 1%.

4.4. Regional differences in carbonate chemistry

The ratio of TA to the dissolved inorganic carbon concentration (TA:~~-~~C_T) is of particular interest because it serves as an indicator of the relative abundance of carbonate species (e.g., HCO_3^- and CO_3^{2-}) in seawater. According to Wang et al. (2013), for a specific temperature and pressure, the CO_2 system parameters, such as the aragonite saturation state and pH value, are closely correlated with this ratio, which has been widely used in studies of seawater carbonate chemistry (Zeebe and Wolf-Gladrow, 2001).

Differences in the seawater TA: C_T imply, for example, differences in buffer intensity, also called buffer capacity (Revelle factor). The buffer intensity of the seawater carbonate system is at a minimum when $CO_3^{2-} \sim CO_{2aq}$, where the TA and C_T concentrations are approximately equal (i.e., when TA: $C_T \approx 1$).

In **Figure 8** (corresponding to the NW region), water with a relatively low salinity (<35) dominates. A linear regression line derived from the SSS=20-37 portion of the TA-SSS plot produced a very low TA.~~–~~ In contrast, in **Figure 8C** (SW region), high SSS values ~~of SSS~~ (>32) are observed in

18

the TA-SSS plot. This region is not affected by major river discharge. The variations in TA and SSS are assigned to physical factors, especially the balance between precipitation and evaporation. The eastern edge (**Figure 8B** and **Figure 8D**) has regions with high productivity associated with the discharge of large rivers, such as the Niger and Congo Rivers. In **Figure 8B,** a very low TA was observed at zero salinity. As indicated in <u>Section</u> ~~section~~ 3.5, low rates of CO_2 consumption have been reported for the Niger and Congo Rivers. As a result, the chemical, geological, biological and physical environments of coastal areas are affected. Low-salinity regions at the eastern edge (SSS <35) in the Atlantic Ocean can be found in two regions according to Bakker et al. (1999): one north of the equator and one near the Congo River. In contrast, in high-salinity offshore waters (>32), TA and SSS exhibited a tight linear correlation with an elevated TA.

The in- situ ~~observation the~~<u>observations of</u> TA and C_T obtained ~~at~~<u>in</u> the coastal ~~region~~<u>regions</u> of Africa and Brazil show significant differences (Bonou et al., 2016b). The biogeochemical composition of each border is different, and many different processes occur at each border, which are different from one another, including in the SSS≥35 regions.

Figure 8

The values observed here showed typical values for tropical waters, with a slight increase in the average values in the TA: CT (SW region; **Figure 9C**).

~~The~~ **~~figure~~ Figure 9B** to **~~figure~~Figure 9D** ~~shows to be~~<u>show a</u> relatively well-buffered TA: C_T > 1.15, while **~~figure~~Figure 9A**~~, indicate~~ <u>indicates</u> a minor buffering capacity (TA:C_T =1.1). A lower buffer capacity may respond to coastal acidification, such as ~~may accompany~~ <u>increases</u> in atmospheric CO_2 or eutrophication events.

19

Biogeochemical processes such as photosynthesis, respiration (P-R), and air–sea CO_2 exchange also change the C_T. Changes in the C_T in regions with high fluvial discharge can alter these processes, and consequently reducingreduce the TA:C_T ratio. In the SW region, TA:CT is high, making conditions more favorable for oceanic uptake of atmospheric CO_2.

Figure 9

5. Conclusions

The tropical Atlantic Ocean receives an important amount of carbon from the African and South American continents, which present different features at their oceanic borders. In this work, the comparative study of TA and C_T data from the coastal region of Africa and Brazil shows significant differences between these variables (Mann–WhitneyMann–Whitney test, α=0.05, p=0.0001). These differences are explained by the differences ofin biological activities, the influence of rivers, and the composition of biogeochemicals in different coastal areas. At the western tropical border, the minimum values of the carbon parameters were obtained, while higher values of the carbon parameters were obtained in the eastern tropical Atlantic border. The biogeochemical composition of each border is different, and many different processes occur at each border. The coastal upwelling process at the eastern border contributes to the higher CO_2 concentrations obtained in the eastern coastal area compared to those obtained at the western edge. This physical process increases the CO_2 parameters in surface water, followed by an additional physical process that transports the rich water masses from the African coast to the Brazilian coast through oceanic circulation (SEC). The river characteristics at each border are different in terms of their physical and biological activities and chemical composition. The existing TA and C_T relationships present spatial limitations, and the use of the empirical TA relationship determined by Lefèvre et al. (2010)

20

~~to~~for the observation data at the eastern border presents high root mean square error values. The similarity between the relationships from Takahashi et al. (2014) and Lefèvre et al. (2010) suggests that calculation of the carbon parameters in the eastern region, using one of these relationships, will lead to a higher root mean square error value. Otherwise, the climatological map determined by Takahaski et al. (2014) in the eastern region using this ~~relation~~relationship may be affected by an important bias compared to that in other regions. On the other hand, the TA relationship determined by Koffi et al. (2010) is not a better relationship to be applied to the coastal data in the Amazon plume. However, we found that their relationship with TA can be extended to the southwestern part, mainly in the SEC region, for data with SSS≥37.

In coastal regions, the biogeochemical composition of each border is different, and many different processes occur at each border, principally regions that include values for SSS<35.

~~Authors~~Author contributions

All authors contributed extensively to the interpretation of the results and to the writing of the manuscript.

21

project, and the EU integrated project CARBOCHANGE (Grant 264879). F. Bonou acknowledges

Conflict of Interest Statement: The authors declare that the research was conducted in the absence of any commercial or financial relationships that could be construed as a potential conflict of interest.

22

List of figures

Figure 1. Routes of the different cruises (55 cruises), indicating the geographical positions of the total alkalinity (TA) samples in the Tropical Atlantic. The red and green colors represent samples collected from the western and eastern tropical Atlantic, respectively, with SSS<35, and the black points are data with SSS≥35 in the tropical Atlantic.

Figure 2. Standard deviation of SSS anomalies for the period from 1970-2013, showing the coastal regions with greater variability in SSS under the influence of rivers.

Figure 3. Monthly distribution of SST (ºC°C) for January and July during the period of 1958-2014 in the tropical Atlantic.

Figure 4. SST climatology of the western and eastern regions for the 1958-2014 period (OAFlux database - http://oaflux.whoi.edu/). NW (-70°ºW to -35°ºW; 0°º to 20°ºN); NE (-35°ºW to +10°ºW; 0°º to 20°ºN); SW (-50°ºW to -15°ºW; 0°º to -20°ºS); SE (-15°ºW to +10°ºW; 0°º to -20°ºS).

Figure 5. Comparisons among: **A**) empirical relationships of Koffi et al. (2010) and Lefèvre et al. (2010) for the estimated TA applied to data with SSS < 35 in the western tropical Atlantic; **B**) empirical relationships of Koffi et al. (2010) and Lefèvre et al. (2010) for the estimated TA applied to data with SSS < 35 in the eastern tropical Atlantic; **C**) empirical relationships of Koffi et al. (2010) and Lefèvre et al. (2010) for the estimated TA applied to data with SSS ≥ 35 in the central tropical Atlantic.

Figure 6. Localization of data with SSS≥37 around Koffi et al. (2010) lines in green and of data with SSS≥35 in black in the central region of the tropical Atlantic.

Figure 7. Annual average data from 10 years (2006-2015) of the chlorophyll-*a* concentrations in the tropical Atlantic Ocean (MODIS-Aqua; 4 km resolution), obtained from: https://giovanni.gsfc.nasa.gov/giovanni/. (Data access: 2017.05.09).

23

Figure 8: TA-SSS relationship in the different ~~sub region~~ subregions in the Atlantic Ocean.

Figure~~:~~ 9: TA:C_T for the NW region (A); NE region (B); SW region (C) and SE region (D). The black line TA:C_T =1; the dashed line ~~indicate~~ indicates the tendency of the observed values. 4.7. C_T and TA normalization in the tropical Atlantic.

Figure 10: C_T bio ($C_{Texcess}$) derived from the mixing model in function SSS (a) in the western region and (b) in the eastern region

Tables

Table 1. Empirical carbon relationships available for the regions near tropical Atlantic Rivers.

REGION	EMPIRICAL RELATION	REFERENCE
Western	TA = 58 * SSS+265	Lefèvre et al. (2010)
	C_T = 50.1*SSS+0.9*(Year-1989) +198	Bonou et al. (2016a)
Eastern	TA = 65.52*SSS+2.50	Koffi et al. (2010)
	C_T = 51.71*SSS-12.79*SST +507.82	Koffi et al. (2010)
Tropical Atlantic	TA = 58.25*SSS+270.9	Takahashi et al. (2014a)

24

Table 2. Additional data cruises used in this paper with measurements of TA and C_T compiled with data from Bonou et al. (2016) for all tropical Atlantic Ocean data.

CRUISE	PERIOD	SHIP	REFERENCE	METHODOLOGY		PRECISION/ ACCURACY	
				TA[a]	C_T	TA (μmol kg⁻¹)	C_T (μmol kg⁻¹)
TTOTASSV	Dec 1982-Jan 1983	*R/V Knorr*	Takahashi et al.(2014b)	-	-	-	-
AJAX_1983	Oct 1983-Fev 1984	*R/V Knorr*	Chipman et al. (2007)	-	-	-	-
SAVE-1	Nov-1987	*R/V Knorr*	Takahashi et al. (1995)	-	-	-	-
SAVE-2	Dec-1987	*R/V Knorr*	Takahashi et al. (1995)	-	-	-	-
SAVE-3	Jan-1988	*R/V Knorr*	Takahashi et al. (1995)	-	-	-	-
WOCE-A16C (SAVE)	Mar-Apr 1989	*R/V Melville*	Takahashi et al. (1989)	-	-	±2/±2	±2/±2
CITHER 1	Jan- Mar 1993	*R/V Atalante*	Oudot et al. (1995)	-	Chromatography	-	-
EGEE-1	Jun-Jul 2005	*R/V Antea*	Koffi et al. (2010)	Full	-	±2/±2	±2/±2
EGEE-2	Sep 2005	*R/V Antea*	Koffi et al. (2010)	Full	-	-	-
EGEE-3	Mai-Sep 2006	*R/V Antea*	Koffi et al. (2010)	Full	-	-	-
EGEE-5	Jun-Jul 2007	*R/V Antea*	Koffi et al. (2010)	Full	-	-	-
EGEE-5	Jun-Jul 2007	*R/V Antea*	Koffi et al. (2010)	Full	-	-	-
EGGE-6	Set 2007	*R/V Antea*	Koffi et al. (2010)	Full	-	-	-
CITHER 2-1	Jan-Mar 1994	*R/V Maurice Ewing*	Rios et al. (2005)	-	SOMMA	±1.2/±1.2	±1.64/±1.6
WOCE-A15	Abr-May1994	*R/V Knorr*	Goyet et al. (1995)	Full	Colorimetry	-	-
METEOR 68/3	Jul-Aug 2006	*R/V Meteor*	Körtzinger & Steinhoff (2012)	Full	SOMMA	-	-
AMT7	Set-Oct 1998	*RRS James Clark Ross*	Lefèvre et al. (2002)	-	SOMMA	-	-
METEOR 80/1	Oct-Nov 2009	*R/V Meteor*	Körtzinger et al. (2012)	Full	SOMMA	-	-
FICARAM_XV	Mar-May 2013	*Hisperides*	Perez et al. (2013)	Full	-	-	-
CARINA.ATL	1999-2004	*Various ships*	This Study	Full	Potentiometry	-	-

[a]**Determined by potentiometric titration, either a full curve ("Full") or a single-point ("1-point") titration. No TA was measured during the AMT7 cruise.**

25

Table 3. Descriptive statistics (minimum as min, maximum as max, mean and standard deviation as STD) of TA and C_T in the eastern region (103 data points) and western region (392 data points).

REGION	TA (μmol kg^{-1})				C_T (μmol kg^{-1})				SSS				SST(°C)			
	Min	Max	Mean	STD	Min	Max	Mean	STD	Max	Min	Mean	STD	Max	Min	Mean	STD
Western	323.0	2372.0	2099.4	286.4	397.7	2075.3	1779.6	236.4	34.9	1.1	31.	4.9	30.5	25.5	28.6	0.8
Eastern	1492.9	2320.7	2198.0	141.9	1389.6	2033.0	1892.2	94.2	34.9	22.9	33.6	2.1	29.1	22.8	27.8	1.2

Table 4. Root mean square error (rmse) of estimated TA and C_T from existing relationships.

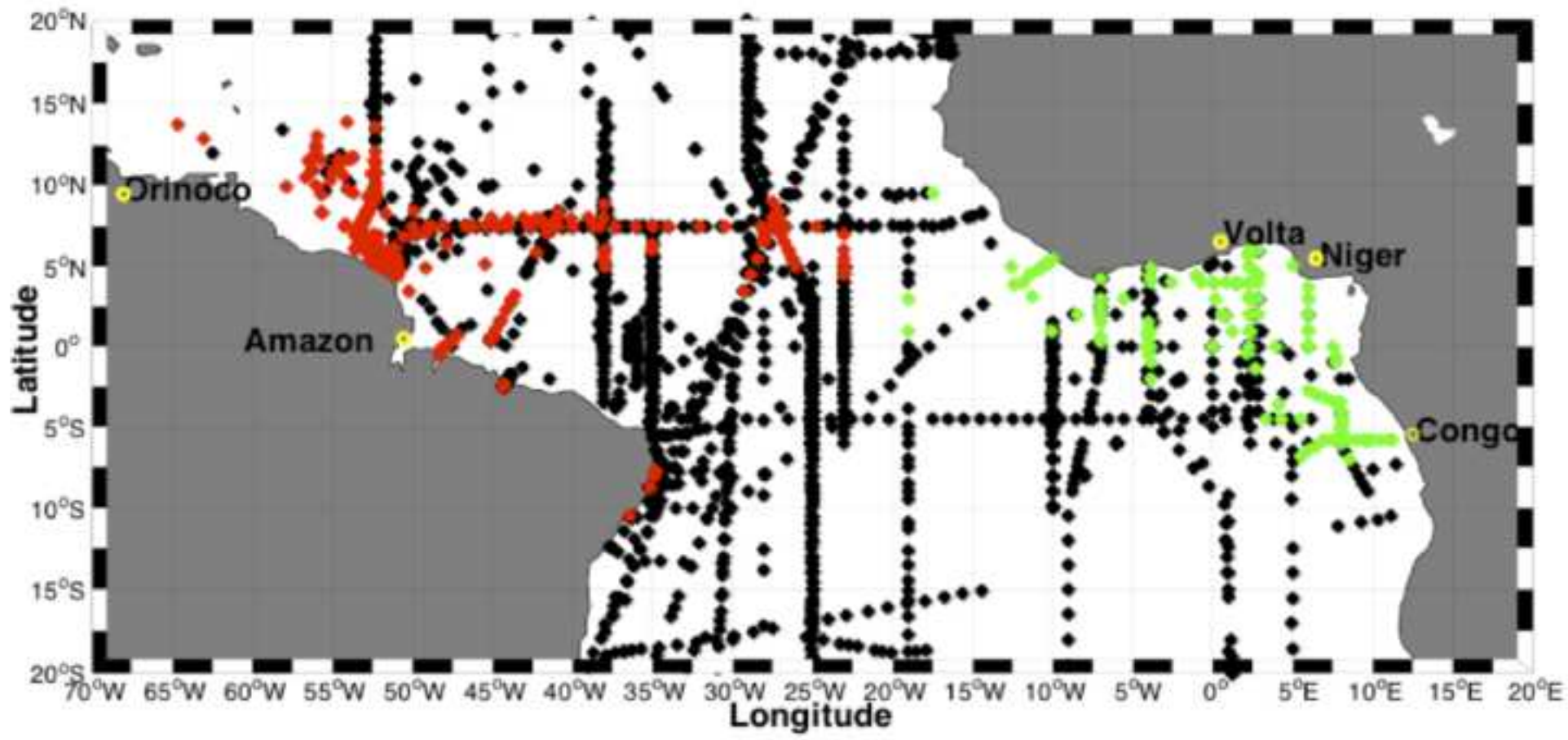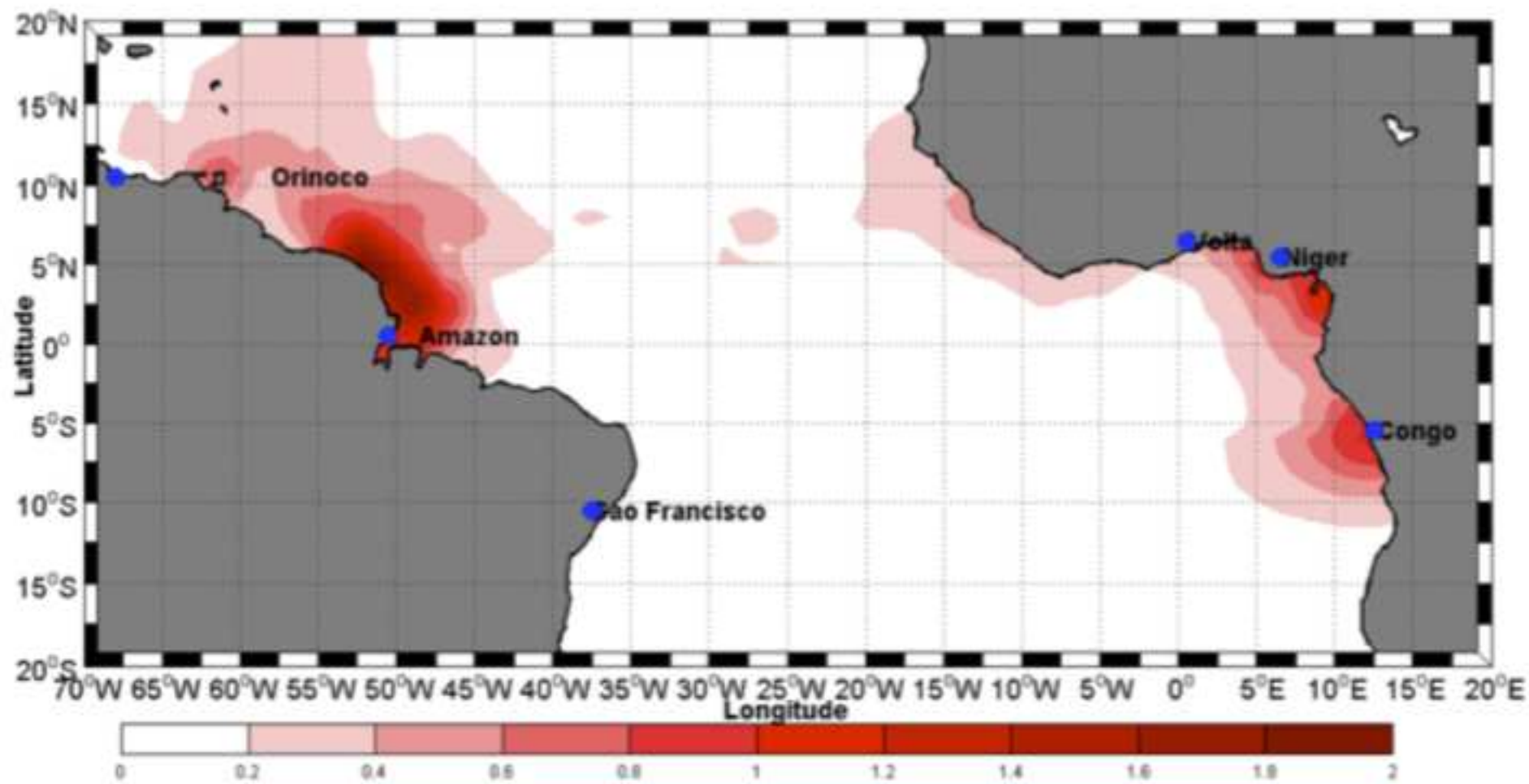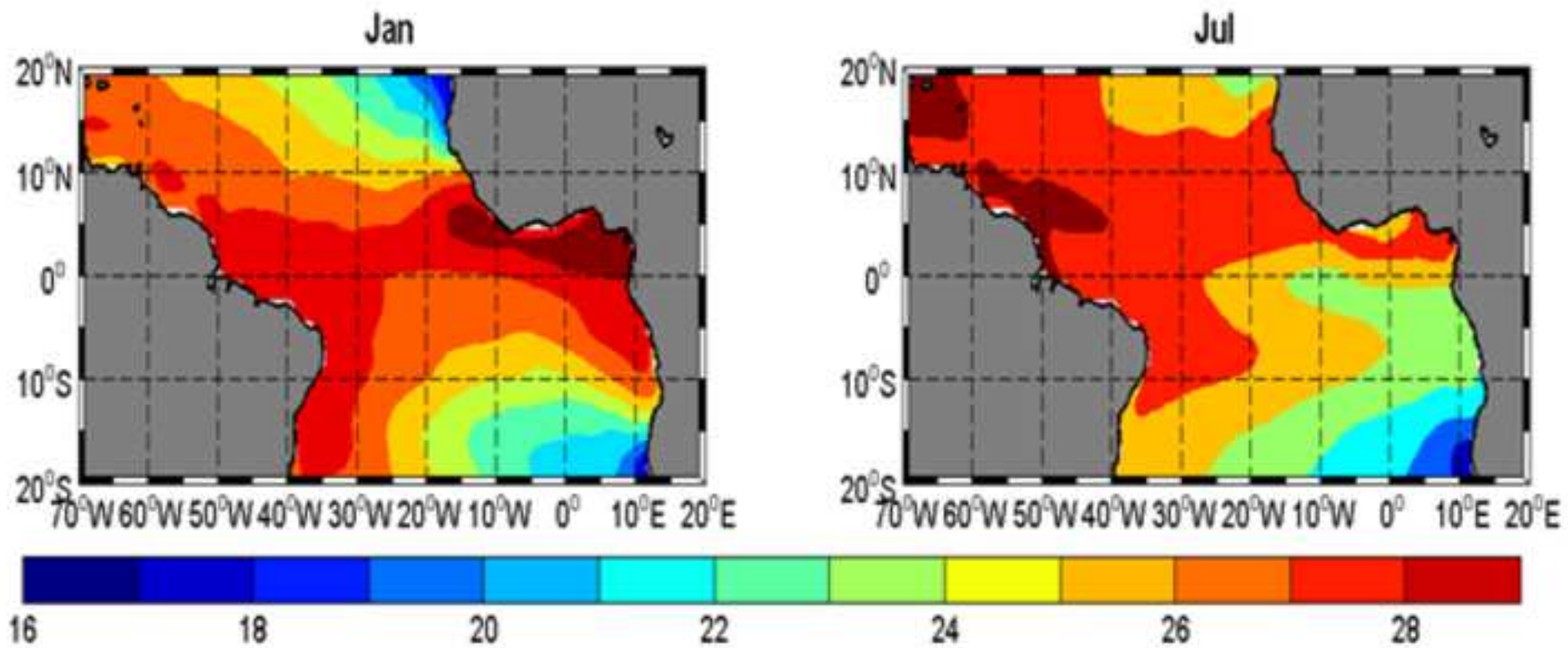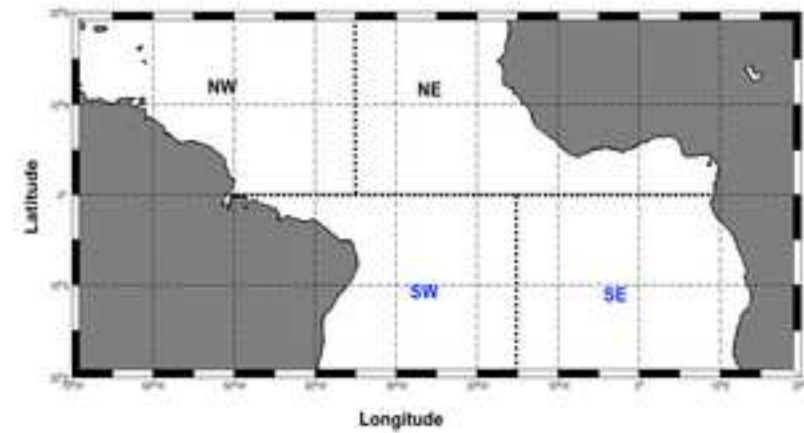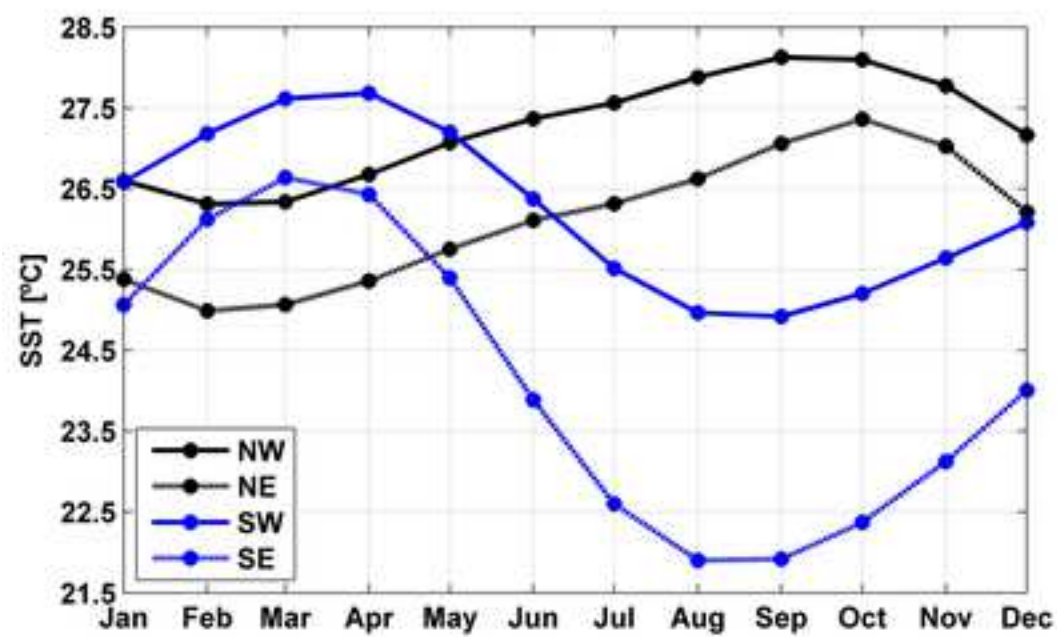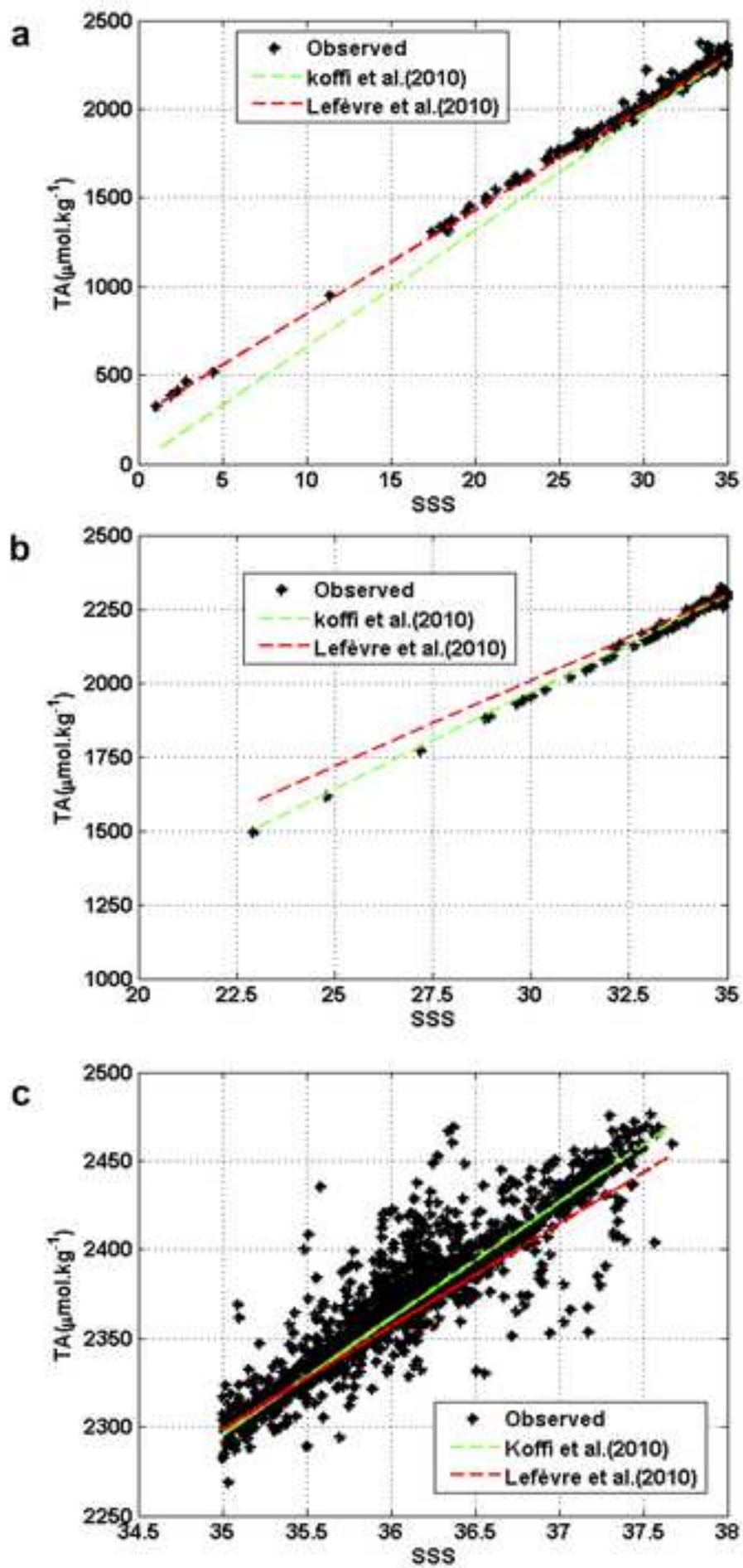| PARAMETER	REGION	N	REFERENCE	RMSE (μmol kg^{-1})
TA	Western (SSS<35)	392	Lefèvre et al. (2010)	28.6
			Koffi et al. (2010)	64.8
	Eastern (SSS<35)	103	Lefèvre et al. (2010)	28.5
			Koffi et al. (2010)	12.5
	Central (SSS≥35)	1848	Lefèvre et al. (2010)	20.5
			Koffi et al. (2010)	19.2
C_T	Western (SSS<35)	392	Bonou et al. (2016a)	41.1
			Koffi et al. (2010)	47.9
	Eastern (SSS<35)	103	Bonou et al. (2016a)	29.6
			Koffi et al. (2010)	28.1
	Central (SSS≥35)	1848	Bonou et al. (2016a)	35.1
			Koffi et al. (2010)	34,7

26

Figure 1

Figure 2

Figure 3

Figure 4

Figure 5

Figure 6

Figure 7

Figure 8
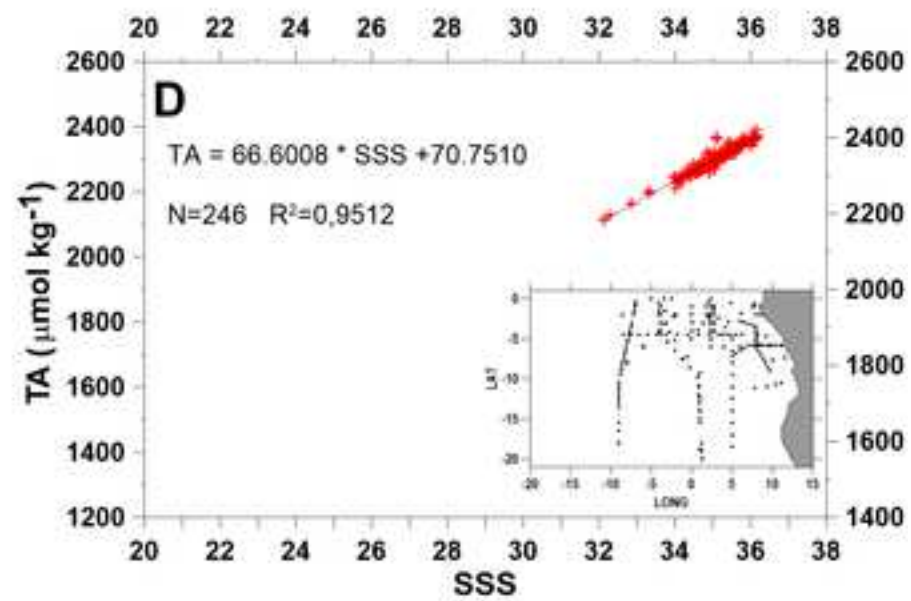
Figure 9

line figure

Western region

PRODUCTIVITY(+)

RESPIRATION(-)

Average of ΔC_T excess=-92 μmol.kg^{-1} (7%)

a)

ΔC_T bio (μmol.kg^{-1})

SSS

Eastern region

PRODUCTIVITY(+)

RESPIRATION(-)

b)

Average of ΔC_T excess= -3 μmol.kg^{-1} (0.2%)

ΔC_T bio (μmol.kg^{-1})

SSS